Preparation and Properties of Polymer Modified Graphene Materials

March 2015

Division of Chemistry for Materials

Graduate School of Engineering

Mie University

Nabihah Binti Abdullah

PREFACE

This work was carried out under the supervision of Professor Fumio Kokai, Division of Chemistry for Materials, Graduate School of Engineering, Mie University, from October 2011 to March 2015.

The main objectives of this thesis are to synthesize and characterize functionalized graphene and graphene-based materials. Functionalized graphene-based materials are expected to widen their promising application.

This thesis consists of three chapters. First chapter of this thesis describes the preparation of graphene flakes by ultrasonication-assisted exfoliation of graphite and characterization of the resulting graphene flakes. The second chapter mentions modification of exfoliated graphene flakes with organic polymer to increase the dispersibility or solubility of the polymer-grafted graphene flakes in a wide variety of solvents. The third chapter deals with hybridization of reduced graphene oxide with silica. A polymer compatibilizer was introduced onto reduced graphene oxide to make it possible to mix with silica.

Table of Contents

Chapter 3 Hybridization of Reduced Graphene Oxide with Silica by Using Poly(2-methyl-2-oxazoline) Modified Reduced Graphene Oxide

3.1 Abstract

3.2 Introduction

3.3 Experimental

3.4 Results and Discussion

3.5 Conclusion

3.6 References

General Introduction

Graphene was first reliably produced in 2004 by Geim and Novoselov at the University of Manchester.[1] Single-atom-thick crystallites (Figure A) were extracted from bulk graphite by lifting graphene layers from graphite with an adhesive tape then transferred them onto a silicon wafer. Graphene is a two-dimensional (2D) form of graphite and consists of a single layer of sp^2 hybridized carbon atoms in a honeycomb lattice. This structure is bringing new properties that are opening up many new opportunities for the one of the oldest elements known. Typically important properties of graphene are high electron mobility (200 000 $cm^2v^{-1}s^{-1}$), [2] high aspect ratio, large surface area (2,630 $m^2\ g^{-1}$),[3] transmittance of visible light (97.7 %),[4] high tensile modulus (1 TPa),[5] high thermal conductivity (5000 $Wm^{-1}K^{-1}$),[6] and good chemical stability. During the last decade a tremendous amount of research has been conducted on graphene from the view point of fundamental science as well as technological applications.

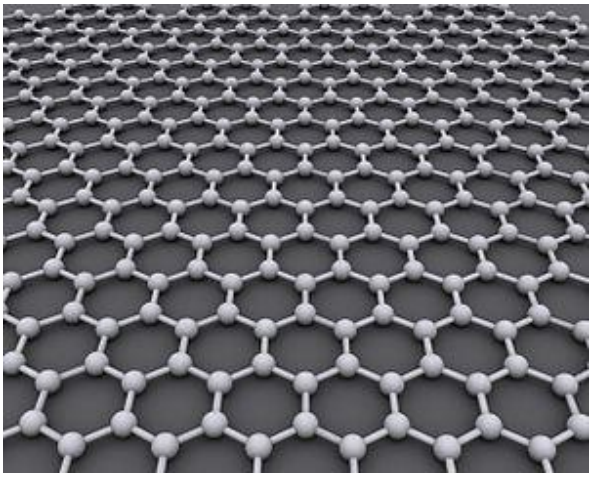

Figure A Graphene made from single-atom thick of graphite

Modification of graphene is one of hottest topics in the field of graphene research. An ideal structure of graphene is a complete two-dimensional crystal, and this inert surface structure also accounts for its chemical stability, large surface energy, weak interactions with other solvents. Thus, graphene is prone to agglomerate irreversibly due to strong van der Waals forces between graphene sheets. In order to obtain a stable dispersion of graphene in solvents, appropriate functionalization of the graphene surface would be virtually important.[7-15] By far, a variety of functionalization methods including covalent and non-covalent modifications has been reported towards improving the solubility of graphene. For covalent modifications of graphene, the resultant products are rather stable. Representative chemical modification of graphene includes radical addition, carbene addition, [2+1]cycloaddition, and aryne cycloaddition[16] (Scheme A).

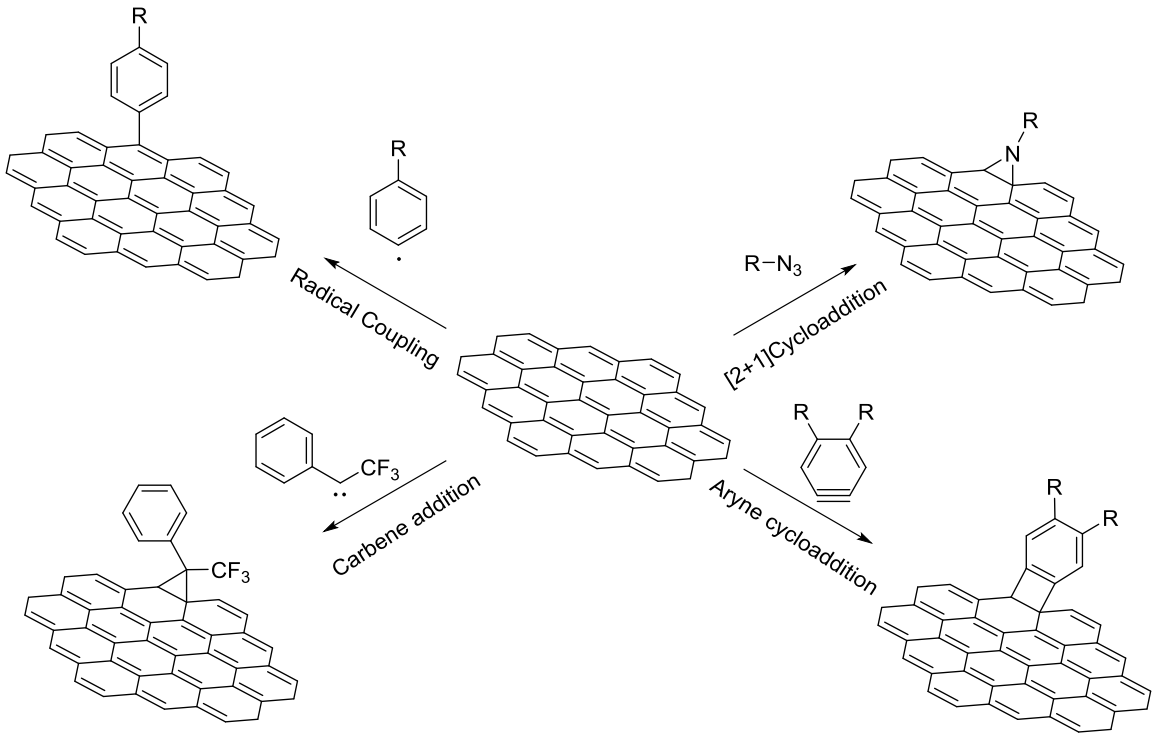

Scheme A Direct functionalization method of graphene

Alternative chemical modification is oxidation of graphite followed by exfoliation to give graphene oxide (Scheme B). The introduced oxygen-containing functional groups (-OH, -COOH, C=O, and epoxy) make it easy to be exfoliated and the resulting graphene oxide shows good dispersibility in water. Further, various chemical modifications are possible by using the functional groups on the surface of graphene oxide.

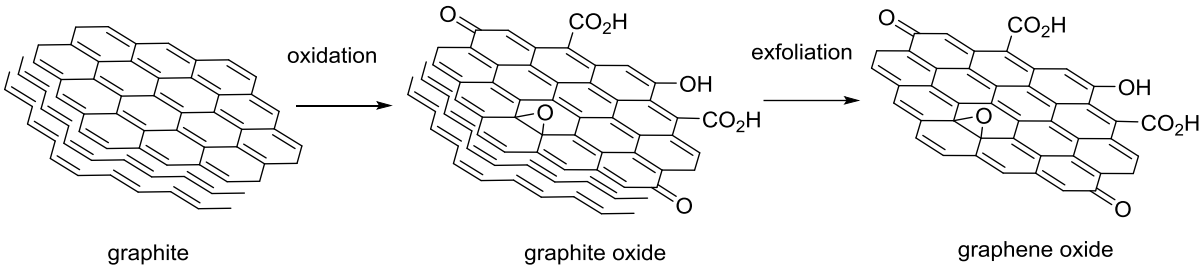

Scheme B Route to synthesize graphene oxide

The purpose of this thesis is to develop novel materials based on graphene through modification of graphene-related compounds. Especially, introduction of well-defined polymers onto graphene via the grafting-on method will be described. In order to explore graphene-based functional materials for various applications, modification of graphene with polymers was carried out to obtain graphene-based fusion materials with solution processability, compatibility with silica, and thermo-responsibility.

References

1. A. K. Geim, K. S. Novoselov. *Nature Materials* **2007**, *6*, 183-191

2. S.V. Morovoz, K.S. Novoselov, M.I. Katsnelson, F. Schedin, D.C. Elias, J.A. Jaszczak, A.K. Geim, *Phy. Rev. Lett*. **2008**, *100*, 016602.

3. M. D. Stoller, S. Park, Y. Zhu, J. An, R. S. Ruoff, *Nano Lett.* **2008,** *8*, 3498-3502.

4. R. R. Nair, P. Blake, A.N. Grigorenko, K.S. Novoselov, *Science* **2008**, *320* , 1308.

5. C. Lee, W.Wei, J. W. Kysar, J. Hone , *Science* 2008, *321*, 385-388.

6. A. A. Balandin, S. Ghosh, W. Bao, I. Calizo, D. Teweldebrhan, F. Miao, C. N.Lau, *Nano Lett.* **2008,** *8* , 902-907.

7. S. Stankovich, R. D. Piner, X. Q.Chen, *J. Mater. Chem*, **2006**, *16*, 155-158.

8. X. L. Li, X. R. Wang, L. Zhang, *Science* **2008**, *319*, 1229-1232.

9. Y. Y. Liang, D. Q. Wu, X. L. Feng, *Adv. Mater*. **2009**, *21*, 1679-1683.

10. A. J. Patil, J. L. Vickery, T. B. Scott, *Adv. Mater*. **2009**, *21*, 3159-3164.

11. C. Xu, X. Wu, J. Zhu, *Carbon* **2008**, *46*, 386-389.

12. S. Wang, P. J. Chia, L. L. Chua, *Adv. Mater*. **2008**, *20*, 3440-3446.

13. S. Niyogi, E. Bekyarova, M. E. Itkis, *J. Am. Chem. Soc*. **2006**, *128*, 7720-7721.

14. J. R. Lomeda, C. D. Doyle, D. V. Kosynkin, *J. Am. Chem. Soc*. **2008**, *130*, 1620-16206.

15. V. Georgakilas, A. B. Bourlinos, R. Zboril, *Chem. Commun*. **2010**, *46*, 1766-1768.

16. J. Park, M. Yan, *Acc. Chem. Res*. **2013**, *46*, 181-189.

Chapter 1

Synthesis and Structure Control of Graphene by Sonication of Graphite Nanoplatelets

1.1 Abstract

Various techniques such as mechanical exfoliation, chemical vapor decomposition and exfoliation of graphite are used to prepare graphene. In this chapter, multi-layered graphene flakes (GFs) were prepared from ultrasonication of graphite nanoplatelets (GNPs) in *N*-methylpyrrolidone (NMP) as a solvent. The study was undertaken to evaluate the effect of ultrasonication on GFs sizes and thicknesses after the exfoliation of GNPs by different powers (310 and 180 W) and time (3–300 min) of ultrasonication. Transmission electron microscopy (TEM) showed the size of the GFs was decreased from 5.4 μm to 2.2 μm after using 180 W of ultrasonication power for 3 min whereas the minimum size is about 0.6 μm after using 310 W of ultrasonication power for 300 minutes. Raman spectroscopy and thermal gravimetric analysis (TGA) were used to investigate the graphitic characteristics and thermal stability of the exfoliated GFs. The ratio of the D band intensity to G band intensity (I_D/I_G) in Raman spectra was low, indication of high quality GFs produced. On the other hand, the ratio of the D band intensity to the 2D band intensity (I_D/I_{2D}) confirmed the thickness of GFs was reduced with increasing time and power of ultrasonication. GFs produced were stable up to 1000 ^{0}C. The GFs produced will be used in the experimentation of Chapter 2.

1.2 Introduction

Graphene has been synthesized in various techniques and on different substrates. The followings are brief summary of the synthesis methods, and comment on their maturity, advantages and disadvantages, and targeted applications.

(1) Mechanical exfoliation

It is known also as scotch tape method. The first single layer graphene was prepared by micromechanical cleavage of highly ordered pyrolytic graphite (HOPG).[1] In this method adhesive tape was used by pressing to the surface of graphite to remove multiple layers of graphene from graphite. By repeating this method, sheets of single layer of graphene finally recovered. It is possible to form a high quality graphene but it is not suitable for large scale production of graphene.

(2) Chemical vapor decomposition (CVD)

It has proved to be one of the best processes for large-scale graphene fabrication and a well-known process in which a substrate is exposed at high temperature. Because the high temperature is not desired in many cases, plasma-assisted decomposition and reaction may lower the process temperature. There are numerous advantages to the thermal CVD process. The process yields high quality and high purity final products in large scale. Moreover, by controlling the CVD process parameters, control over the morphology, crystallinity, shape, and size of the desired product is possible.

(3) Graphite Oxide Exfoliation

Oxidation of graphite with a strong acid and an oxidizing agent has been studied for over a century and a half. By reacting graphite with such reagents, a variety of covalently bonded oxygen functionalities can be added throughout he graphite. This increases the interplanar spacing and causes the material to become more hydrophilic. This oxidized graphite can be exfoliated and reduced chemically,[2] thermally[3] or electrochemically ,[4] to form single sheets. The final product from oxidation and reduction of graphite has residual functional groups that change the properties of the individual graphene sheets, but currently this is considered to be one of the most practical approaches to graphene sheet isolation.

However, graphene oxides (GO) facing some significant disadvantages. Due to disruption in the π-orbital structure on oxidation, GO is a poor electrical conductor. The oxides can be removed resulting in a significant increase in conductivity. In addition, thermal reduction is most successfully carried out at ~1000°C, a temperature which unsuitable for many applications.

(4) Exfoliation of Graphite

Graphite can be successfully exfoliated in liquid environments by exploiting ultrasound to extract individual layers. The liquid-phase exfoliation process typically involves three steps: (1) dispersion of graphite in a solvent (2) exfoliation and (3) purification. Graphene flakes can be produced by surfactant-free exfoliation of graphite via chemical wet dispersion, followed by ultrasonication in organic solvents. Successful exfoliation requires the overcoming of the van der Waals attractions between the adjacent layers. During ultrasonication, shear forces and cavitations, i.e. the growth and collapse of micrometer-sized

bubbles or voids in liquids due to pressure fluctuations. This process produces intense local heating, high pressures, enormous heating and cooling rates and liquid jet streams. Different solvents have been used for graphite exfoliation. Solvents with surface tension $\gamma \sim 40$ mJm^{-2} are the best solvents for the dispersion of graphene and graphitic flakes, since they minimize the interfacial tension between solvent and graphene. Examples of the solvents are *N*-methyl-2-pyrrolidone (NMP), *ortho*-dicholorobenzene (*o*-DCB) and *N*,*N*-dimethylformamide (DMF).

The rise of interest towards graphene and the needs of high volume of graphene for applications such as composites lead to the investigation of large scale production. Among various methods for graphene formation, the exfoliation of graphite in liquid phase gives a promising route to produce graphene-like materials.[5] In this research NMP was chosen as a solvent because the surface tension is close to 40 mJm^{-2} and suitable for direct exfoliation of graphene.[6] In this work, we will demonstrate that graphene can be exfoliated from GNPs using NMP as the solvent and ultrasonic treatment. It is important that this method is no-oxidative and does not require high temperature process. Furthermore, it is involving simple preparation, starting with safe and low cost material.

1.3 Experimental

Materials

Graphite nanoplatelets (GNPs) were purchased from XG Science USA (5.6 µm nominal average size and 5-10 nm (15-30 layers) thickness). NMP was purchased from Nacalai Tesque.

Preparation of Multi-Layered Graphene Flakes (GFs)

GNPs (50 mg) were added into a sonication glass tube that contained 50 mL of NMP. The dispersion was deoxygenated for 30 min by bubbling with N_2 to reduce the defect of GFs produced due to the ultrasonication. It was then ultrasonicated (Figure 1.1) using the bath ultrasonic processor (Nanoruptor-350) at 11 °C, 180 W and 310 W between 3 - 300 min. After the ultrasonication, 50 mL of ethanol was added to the reaction mixture, and the mixture was centrifuged (CN-2060 by AS ONE) for 1 h at 5000 rpm.

After the centrifugation process, graphene sediments were attached to the wall of the vials separated from liquid. Remove the liquid and the resulting sediments were then dried at 70 °C for about 1 h to evaporate ethanol. Exfoliated GFs were obtained as black sediment (45-48 mg).

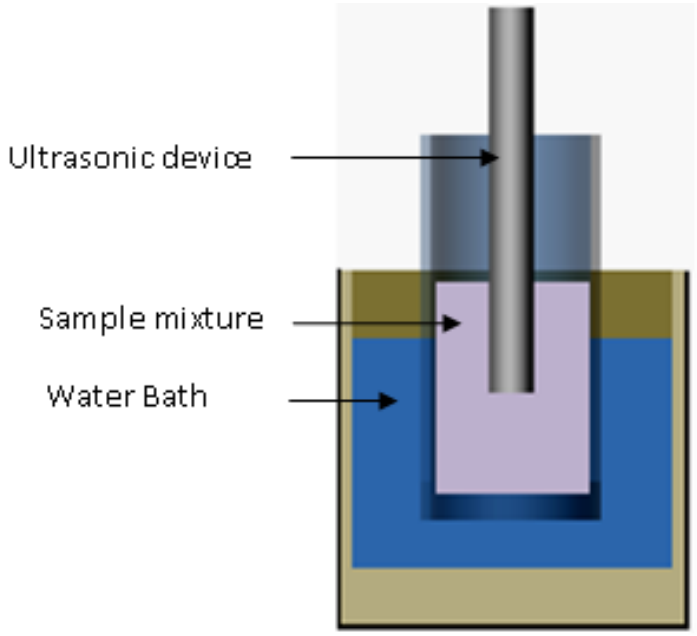

Figure 1.1 Cross-sectional image of ultrasonication set-up.

Measurements

The morphology of sediments was investigated using transmission electron microscope (TEM, Hitachi H-7000) operating at 100 kV. The quality of exfoliated GFs was determined by using Raman spectroscopy and thermal gravimetric analysis; TGA (SII EXSTAR 6000). The Raman spectroscopy (Horiba XploRa) had an excitation wavelength of 488 nm. TGA was performed by heating samples at least more than 5mg for each condition from 30 ºC to 1000 ºC at a heating rate of 10 ºC/min under nitrogen atmosphere (constant 300 mL/min N_2 flow) using alumina as the sample pan.

1.4 Results and Discussion

Transmission Electron Microscopy (TEM)

The morphological properties of GNPs and GFs had been observed using TEM. Figure 1.2 shows the images of GNPs before and after ultrasonication. As the time increased, the thickness and size of the GFs were reduced. The average size of GNPs was 5.4 µm. GNPs were composed from many layers of graphene, thus the dark colour of TEM image in Figure 1.2a indicates GNPs were thicker compared to exfoliated GFs (Figures 1.2b and 1.2c). The images of GFs were brighter in contrast with GNPs proving that the number of layers decreased after being ultrasonicated. The average size of GFs was 2.2 µm (180 W, 3 min) and 0.6 µm (310 W, 300 min).

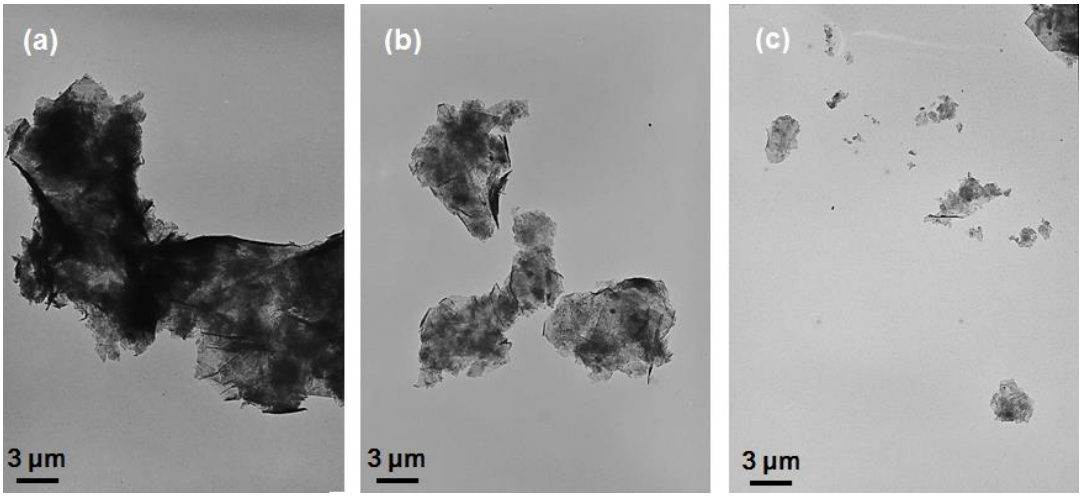

Figure 1.2 TEM image of (a) GNPs, (b) GFs (180W, 3 min), and (c) GFs (310W, 300 min).

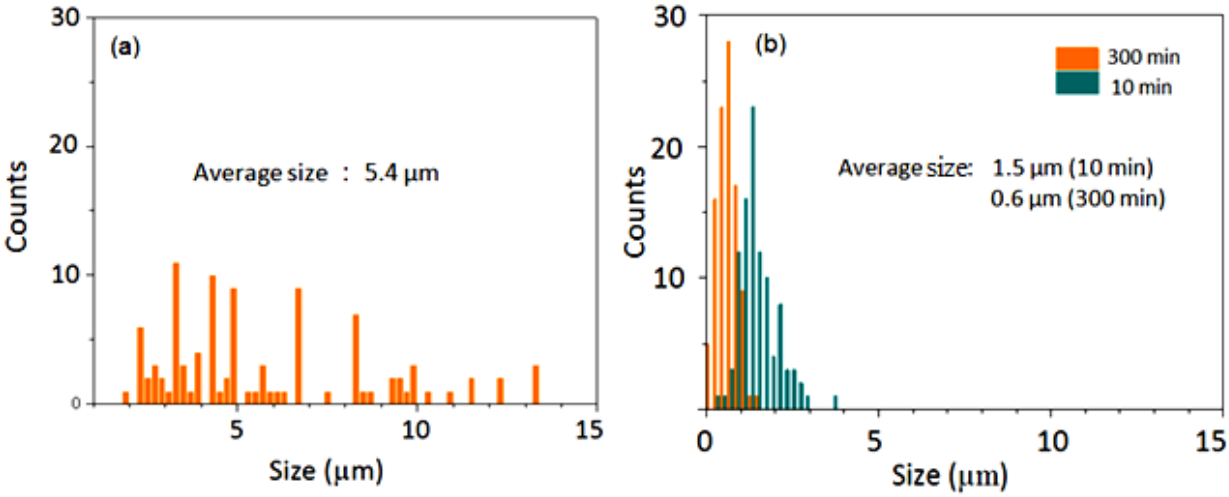

Figure 1.3 Histogram of size distributions of (a) GNPs and (b) GFs ultrasonicated at 310 W for 10 and 300 min.

Figure 1.3 shows size distributions of starting material, GNPs and GFs, which were estimated by evaluating 100 samples for each condition. The size distributions of GNPs were varied between 1.9 μm to 13.3 μm. The average size of GNPs was 5.4 μm. After ultrasonication at 310 W (Figure 1.3b) the average size of GFs was decreased to 1.5 μm and 0.6 μm for 10 and 300 minutes respectively. Longer ultrasonication times resulting in smaller size of GFs.

XRD Analysis

Figure 1.4 shows the XRD patterns for GNP and GFs. The peaks show are sharp and intensively at $2\theta=26.5^{\circ}$ corresponding to (002) plane, representing organized crystal structure with interlayer spacing of 0.34 nm.[7] This is because the interlayer spacing inside the few-layered graphene sheet has a structure similar to that of normal graphite. (002), (101) and (004) plane can be observed in GNPs and GFs ultrasonicated at 180 W for 3 min. However, (001) plane has disappeared due to increasing power and time of ultrasonication.

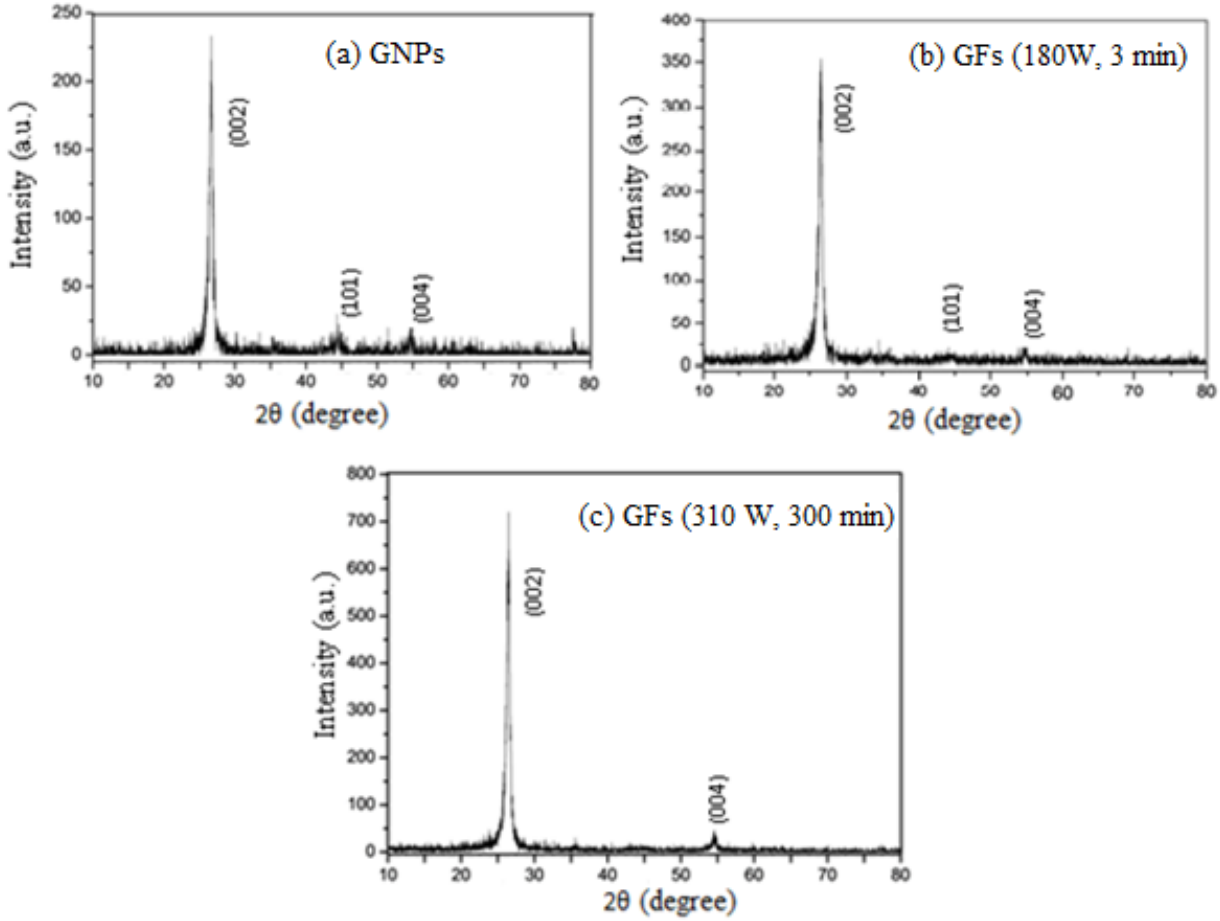

Figure 1.4 XRD patterns of (a) GNP, GFs produced by ultrasonication at power of (b) 180W, 3min and (c) 310 W, 300 min

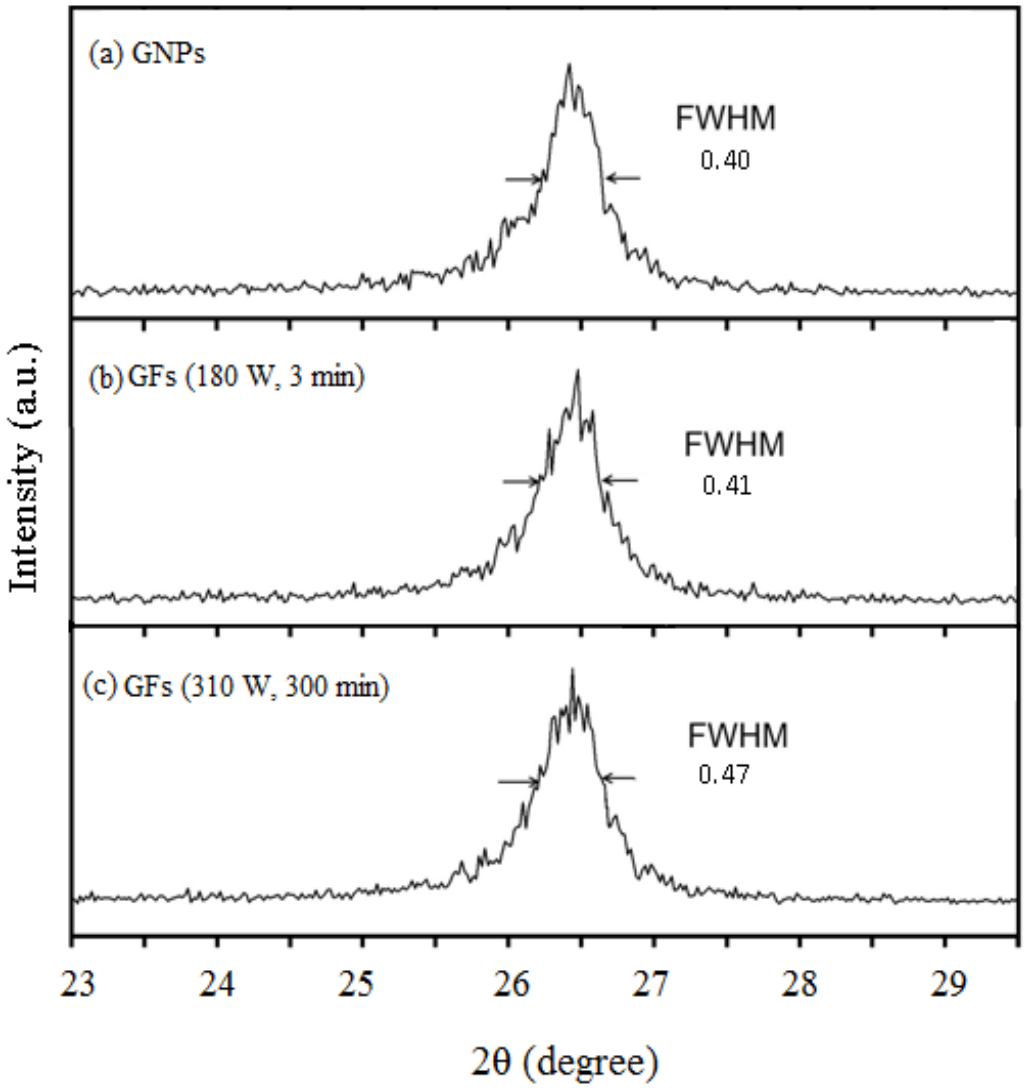

Figure 1.5 FWHM of (002) plane of (a) GNPs , GFs ultrasonicated at (b) 180 W for 3 min and (c) 310 W for 300 min

Figure 1.5 shows the enlarged view of the (002) plane's peaks of GNPs and GFs at 2θ =26.5º. The value of full width at half maximum (FWHM) has increased from 0.40 to 0.47 for GNPs and GFs ultrasonicated at 310 W for 300 min. Even though the FWHM changes were small but the broaden peaks might be due to the thinner graphene layers because of high degree of exfoliation. This resulting in new lattice structure that is different from GNPs.[8]

Raman Spectroscopy

Raman spectroscopy is a fast and non-destructive analysis tool which provides high-throughput and unambiguous identification of the properties of graphene films with three most intense peaks: Disorder-related D peak at ~1350 cm^{-1}, the G peaks at ~1590 cm^{-1} and 2D (or G') peak at ~2700 cm^{-1}, respectively. The D band usually provides the information on defects in the crystalline structure of graphene layers, G band is for in plane vibration of sp^2 carbon atom while the 2D band for stacking order (number of layers).[9]

Based from Figure 1.6, D band and G band show the same pattern of good quality graphene.[5,10] The intensity ratios of the D band to the G band are low, indication that the GFs produced were good quality. These ratios are corresponding with the average density of defects.

The 2D band patterns can identify layers number of GFs. However, for more than 5 layers GFs, the Raman spectra become hardly distinguishable from that of bulk graphite.[11] Thus Raman spectra can clearly identify a single layer, from bilayer from few layers (less than 5). This explains why our multi-layered graphene flakes failed to identify this feature. However, the area ratio of the G band to 2D band (I_G/I_{2D}) can be used to indicate the thickness of GFs. The higher ratio indicates to the thicker graphene.[12] The ratios decreased as the time of ultrasonication increased from 3–300 min as shown in Figure 1.7. The ratio was reduced from 1.23 to 1.12 and 1.2 to 1.04 for 180 W and 310 W of ultrasonication power respectively. Using ultrasonication power of 310 W shows more significant difference compared to 180 W. Based on these values we can conclude that the GFs produced were thinner with high power of ultrasonication.

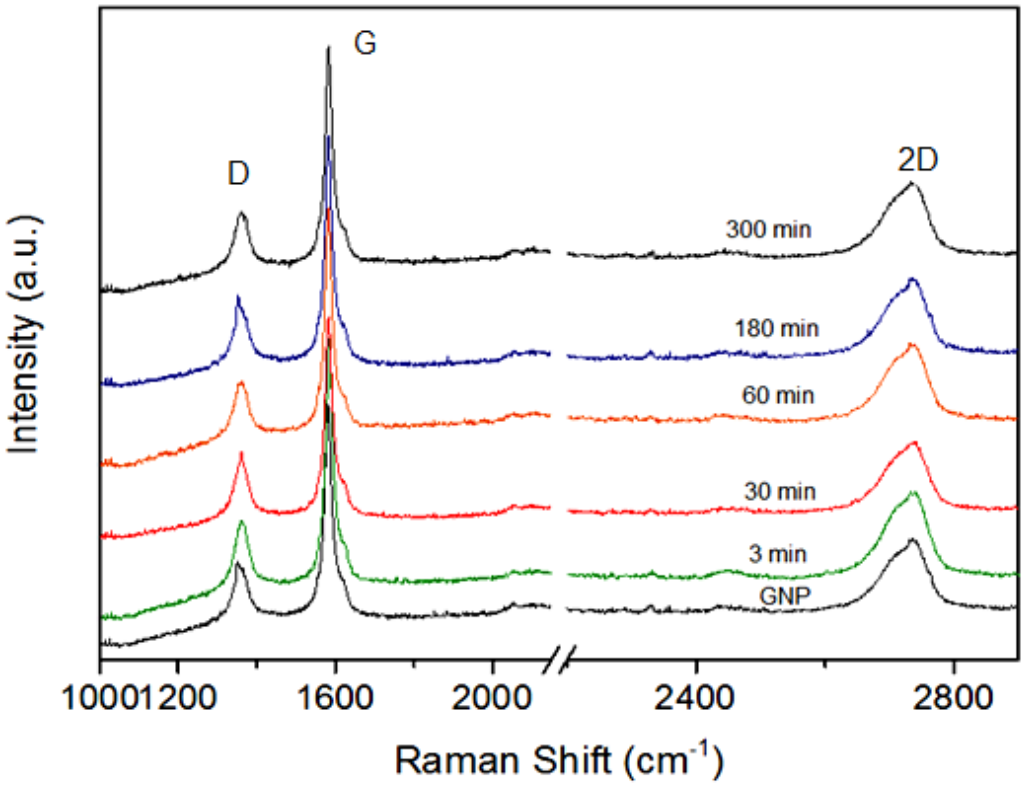

Figure 1.6 Raman spectra of GFs ultrasonicated at 310 W from 3 – 300 minutes.

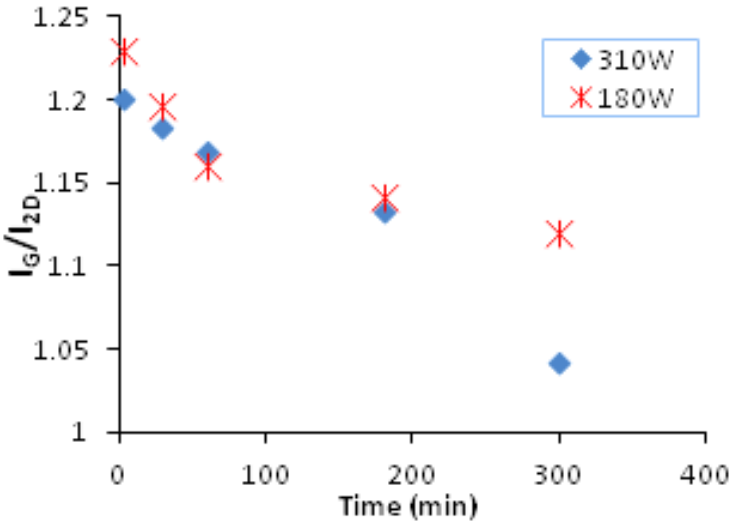

Figure 1.7 Area ratios of G band and 2D band (I_G/I_{2D}) of GFs produced using 310 W and 180 W of ultrasonication.

Thermal Gravimetric Analysis (TGA)

TGA was utilized to investigate the thermal stability of carbonerous materials. The disordered or amorphous carbon tended to be oxidized at around 500 °C due to the lower activation energies for oxidation. However a well graphitized structure started to oxidize at higher temperature around 800 °C.[13] The GFs can be said to start the degradation temperature at 100 °C related to the removal of physically adsorbed water.[14] Figure 1.8 shows the TGA curves of GNPs and GFs in nitrogen atmosphere. Both GNPs and GFs show good thermal stability towards increasing of temperature up to 1000 °C. The final weight loss of GFs was about 8%.

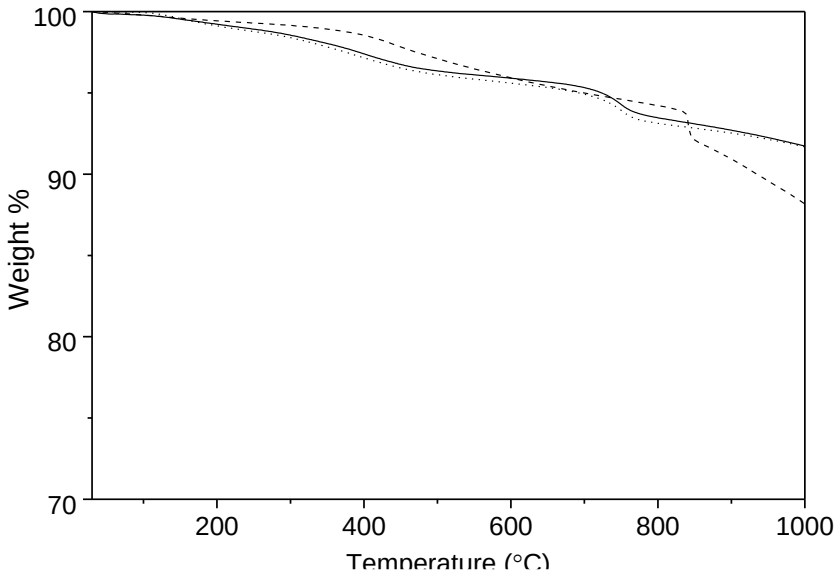

Figure 1.8 TGA curves of GNPs (dashed line), GFs produced by ultrasonication at power of 310W (solid line), and 180W (dotted line). GFs were ultrasonicated at 300 min.

1.5 Conclusion

Based on TEM images of GFs, it can be concluded that the size and the thickness of GFs were decreased when ultrasonication time was increased. Raman spectra showed good quality GFs produced even with increasing time of ultrasonication. The thickness of GFs was reduced with increasing time and power of ultrasonication. Finally, TGA curves showed that the GFs were stable with increasing of temperature in nitrogen atmosphere up to 1000 °C. The GFs produced were used in next experiment in Chapter 2.

1.6 References

1. K. S. Novoselov, A. K. Geim, S. V. Morozov, *Science* **2004** , *306* , 666–669.
2. S. Park, J. An, J. R. Potts, A. Velamakanni, S. Murali, R. S. Ruoff, *Carbon*. **2011**, *49*, 3019–3023.
3. H. C. Schniepp, J. L. Li, M. J. McAllister, *J. Phys. Chem. B* **2006**, *110*, 8535–8539.
4. Z .Wang, X. Zhou, J. Zhang, F. Boey, H. Zhang, *J. Phys. Chem. C* .**2009**, *113*, 14071–14075.
5. Y. Hernandez, M. Lotya, V. Nicolosi, F. M. Blighe, S. De, G. Duesberg, J. N. Coleman, *J. Am. Chem. Soc*. **2009**, *131*, 3611–3620.
6. Y. Hernandez, M. Lotya, V. Nicolosi, F. M. X. Zhang, A. C. Coleman, N. Katsonis, W. R. Browne, B. J. van Wees, B. L. Feringa, *Chem. Commun*. **2010**, *46*, 7539-7541.
7. Y. Wu, B. Wang, Y. Ma, Y. Huang, N. Li, F. Zhang,.Y. Chen, *Nano Res.* 2010, *3*, 661–669.

8. L.Y. Meng, S. J. Park, *J. Colloid Interface Sci.* **2012**, *386*, 285-290.

9. Z. Ni, Y. Wang, T. Yu, Z. Shen, *Nano Res*. **2008**, *1*, 273-291.

10. U. Khan, A. O'Neill, M. Lotya, S. De, J. N. Coleman, *Small* **2010**, *6*, 864–871.

11. A. C. Ferrari, J. C. Meyer, V. Scardaci, C. Casiraghi, M. Lazzeri, F. Mauri, S. Piscanec, D. Jiang, K. S. Novoselov, S. Roth, A. K. Geim, *Phys. Rev. Lett*. **2006**, *97*, 18741.

12. M. Choe, B. H. Lee, G. Jo, J. Park, W. Park, S. Lee ,W. K. Hong, M. J. Seong, Y. H. Kahng, K. Lee, T. Lee, *Organic Electronics* **2010**, *11*, 1864–1869.

13. C. C. Teng, C. C. M. Ma, C. H. Lu, S. Y. Yang, S. H. Lee, M. C. Hsiao, M. Y. Yen, K. C. Chiou, T. M. Lee, *Carbon* **2011**, *49*, 5107 –5116.

14. G. Gedler, M. Antunes, V. Realinho, J. I. Velasco, *Polymer Degradation and Stability* **2012**, *97*, 1297-1304.

Chapter 2

Solubilization of Graphene Flakes through Covalent Modification with Well-Defined Azido-Terminated Poly(ε-caprolactone)

2.1 Abstract

A well-defined poly(ε-caprolactone) (PCL) with terminal azido group was prepared. Grafting-on reaction between the azido-terminated PCL (N_3-PCL) and ultrasonication-assisted exfoliated graphene flakes (GFs) was carried out to obtain PCL-grafted-graphene flakes (PCL-*g*-GFs) which were soluble in a wide variety of organic solvents. GPC, ^{1}H NMR, IR, Raman, UV-vis, and TEM measurements indicated that PCL chains were covalently introduced on the surface of GFs without disrupting the structure of GFs.

2.2 Introduction

Graphene has attracted widespread attention due to its unique properties such as high surface area, excellent thermal and electrical conductivities, and strong mechanical strength.[2-5] Graphene-based nanomaterials have many promising applications in energy-related and environmental-related areas. For instance, in energy-related areas, modified graphene materials have been used in photovoltaic cells,[6,7] lithium ion batteries,[8,9] supercapacitors,[10] and fuel cells.[11] In the environmental remediation area, some graphene-based materials have been used for the degradation of toxic organic pollutants and as sensor devices for pollutant analysis.[12,13] Despite the many potential applications that graphene promises to offer, the limited solubility of graphene due to the strong π-π interaction limits the exertion of its great

potentials. Materials with solution processability and good film-forming property have a number of applications for low-cost device fabrications.

Various efforts have been made to prepare soluble graphene/polymer composites by modification of graphene with organic polymers due to its incredible variety of chemical structures available.[14-16] We are interested in poly(ε-caprolactone) (PCL) as a polymer segment for a graphene/polymer composite. Since PCL is biodegradable and biocompatible polyester with a number of potential applications, PCL-functionalized graphene is expected to find use in biomedical materials, biomedical engineering, biosensor, and materials for drug delivery system. To the best of our knowledge, most of the covalent modification of graphene with PCL reported in the literatures are based on grafting-from method using graphene oxide (GO) as a starting material.[17-19] The grafting-from modification involves two reaction steps composed of introduction of OH groups onto GO surface, followed by *in situ* ring-opening polymerization of ε-caprolactone (CL). Such prepared PCL-functionalized GO may contain some defect structures arising from multistep reactions (oxidation, hydrolysis, and ring-opening polymerization). Further, it is necessary to reduce GO to graphene-like sheets by removing the oxygen-containing groups to restore a conjugated structure.

In this work we examined one-step functionalization of multi-layered graphene flakes (GFs) with preformed azido-terminated PCL (N_3-PCL) to obtain PCL-grafted-graphene flakes (PCL-*g*-GFs) as shown in Scheme 2.1. This method does not need restoration of graphene from GO. The key reaction is nitrene chemistry to introduce PCL macromolecules on GFs. The thermally generated nitrene radicals from azido groups possess high reactivity and can attack the double bonds in carbon nanomaterials such as fullerenes, carbon nanotubes and graphenes to form the covalent bonds of C-N.[20-22]

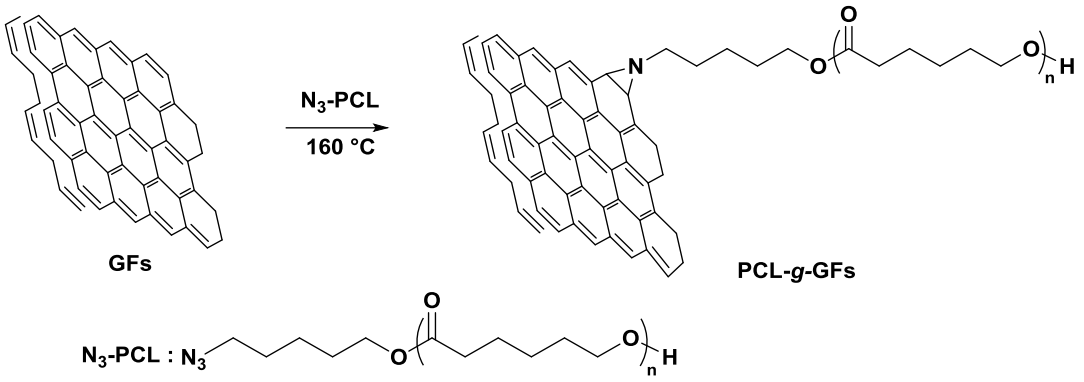

Scheme 2.1 Grafting-on reaction of GFs with PCL.

2.3 Experimental

Materials

Graphite nanoplatelets (GNPs) (nominal average size, 5 μm; thickness, 5–10 nm) were purchased from XG Sciences, USA. 5-Azido-1-pentanol was prepared according to the reported procedure.[23] ε-Caprolactone (CL) (Tokyo Kasei Kogyo, Japan) was distilled over CaH_2 under reduced pressure. All other reagents were purchased from commercial sources and purified by conventional method.

Measurements

^{1}H NMR spectra were recorded at room temperature on a JEOL α-500 nuclear magnetic resonance spectrometer. Samples were dissolved in $CDCl_3$ and tetramethylsilane (TMS) was used as the internal standard. Infrared and UV-vis spectra were recorded on a JASCO FT/IR-4100 and Shimadzu UV-2550, respectively. Thermo gravimetric analysis (TGA) was performed with SII EXSTER-6000 under N_2 gas flow. The heating range was extended from 30 °C to 1000 °C, and the heating rate was 10 °C/min. Gel permeation chromatography (GPC) was carried out on a Tosoh HLC-8020 chromatograph equipped with a set of

polystyrene gel columns (Tosoh TSK gel G2500H + G3000H) and refractive/ultraviolet dual mode detectors. Tetrahydrofuran (THF) was used as the eluent at a flow rate of 1.0 mL/min. The calibration curves for GPC analysis were obtained using polystyrene standards. Matrix-assisted laser desorption/ionization time-of-flight mass spectroscopy (MALDI-TOF MS) was performed with a Shimadzu Kompact II spectrometer in the linear mode with an acceleration voltage of 20 kV. The sample solution was prepared by the dissolution of polymer (1 mg) in 1 mL of THF. The matrix solution was prepared by the dissolution of α-cyano-4-hydroxycinnamic acid (23 mg) in 1 mL of THF. Matrix and polymer solutions were mixed in a 1/1 ratio. To aid sample ionization, the MALDI target was pre-spotted with 0.5 μL of a 0.1 mmol/mL solution of silver sodium iodide in THF and allowed to dry at room temperature. A 0.5–1.0 μL aliquot of the polymer/matrix mixture was deposited on top of ionization agent and air-dried. The morphology of the graphene flakes was observed using a HITACHI H-800 transmission electron microscope operated at 100 kV. Raman spectra were recorded on a Horiba XploRa with an excitation wavelength of 638 nm and a beam spot size of 1-2 μm.

Preparation of N_3-PCL

Into a solution of 5-azido-1-pentanol (0.20 g, 1.6 mmol) and CL (4.4 g, 39 mmol) in 15 mL of toluene was added diphenyl phosphate (0.40 g, 1.6 mmol) in a glove box. The reaction mixture was stirred under an argon atmosphere for 5 h at room temperature. The polymerization was quenched by the addition of Amberlyst A21. The polymer was isolated by precipitation in cold methanol/hexane. The obtained polymer was further purified by silica gel column chromatography using a mixture of ethyl acetate and hexane (2:1 by volume) to give 3.0 g (65%) of N_3-PCL as a white solid. M_n (NMR) = 2500; M_n (GPC) = 3270; M_w/M_n (GPC) = 1.5; IR (KBr): ν = 2945 (s), 2866 (s), 2100 (w), 1728 (s), 1186 cm^{-1} (s); ^1H NMR (500 MHz, $CDCl_3$, δ): 4.06 (t, J = 5.8 Hz), 3.66 (t, J = 6.4 Hz), 3.29 (t, J = 6.8 Hz), 2.31 (t, J = 6.4 Hz), 1.7-1.6 (m), 1.4-1.3 (m).

Preparation of PCL-grafted Graphene Flakes (PCL-g-GFs)

The mixture of freshly-prepared GFs (20 mg), N_3-PCL (20 mg) and NMP (10 mL) was stirred thoroughly for 15 minutes under nitrogen bubbling and heated at 160 °C for 24 h under nitrogen atmosphere. When the reaction was finished, it was cooled to room temperature. After centrifugation (1000 rpm, 30 min) to remove unreacted graphene flakes, the supernatant was filtered with TEFLON filter (0.45 μm) and poured into IPE to precipitate 29 mg of crude PCL-*g*-GFs. The obtained crude product was then dispersed in ether to remove the unreacted N_3-PCL to give 22 mg of PCL-*g*-GFs as a dark brown solid. M_n (GPC) =12000. M_w/M_n (GPC) = 1.3. IR (KBr, cm^{-1}): ν = 2946 (s), 2864 (s) 1730 (s), 1185 (s). ^1H NMR (500 MHz, $CDCl_3$, TMS) δ (ppm): 4.06 (t, J = 5.8 Hz) ($COCH_2CH_2CH_2CH_2CH_2O$), 3.66 (t, J = 6.4 Hz) (-CH_2-OH), 3.6-3.4 (-CH_2-N), 2.31 (t, J = 6.4 Hz) ($COCH_2CH_2CH_2CH_2CH_2O$), 1.7-1.6 (m) ($COCH_2CH_2CH_2CH_2CH_2O$), 1.4-1.3 (m) ($COCH_2CH_2CH_2CH_2CH_2O$).

2.4 Results and Discussion

Preparation of N_3-PCL

The methodology for one-step covalent modification of GFs with PCL is based on grafting-on reaction. Among various chemical reactions for attaching polymers onto graphene, nitrene chemistry is considered to be a useful means to covalently modify graphene and other nanocarbons because only nitrogen molecule generates as a by-product. We prepared a well-defined N_3-PCL via the controlled/living ring-opening polymerization of CL with diphenyl phosphate as an efficient organocatalyst developed by Kakuchi et al.[24]

Well-defined structure of N_3-PCL was confirmed by MALDI-TOF MS as shown in Figure 2.1. The degree of polymerization was designed to be around 20. These short polymer chains should be sufficient to control the solubility of the attached GFs. Moreover, the low molecular weight simplifies characterization such as IR, NMR, and MALDI-TOF MS analysis. Each peak in the spectrum represents N_3-PCL which was cationized by the attachment of sodium cation. For example, the highest peak (m/z = 2549.2) corresponds to N_3-PCL with degree of polymerization of 21. It was noted that there existed two different series of peaks. The molecular weight of the minor series was smaller than that of the major series by 28 Da, indicating the fragmentation of the azido functionality via expulsion of N_2 during MALDI process.[25]

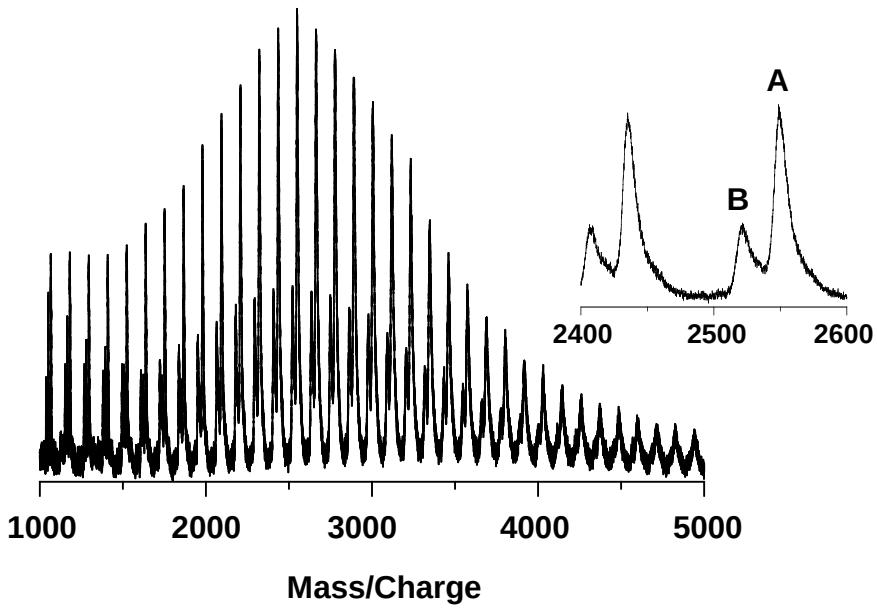

Figure 2.1 MALDI-TOF MS of N_3-PCL.

Further characterization of N_3-PCL was done by using IR and ^{1}H NMR spectra. The IR spectrum of N_3-PCL shows an adsorption peak at 2100 cm^{-1}, which is characteristic of azide

group (Figure 2.2). This is a proof that the synthesis of N_3-PCL was accomplished. The peaks at 2946 cm^{-1}, 2865 cm^{-1} and 1730 cm^{-1}, characteristic of asymmetric and symmetric stretching of CH and carbonyl stretching of PCL (C=O), respectively.

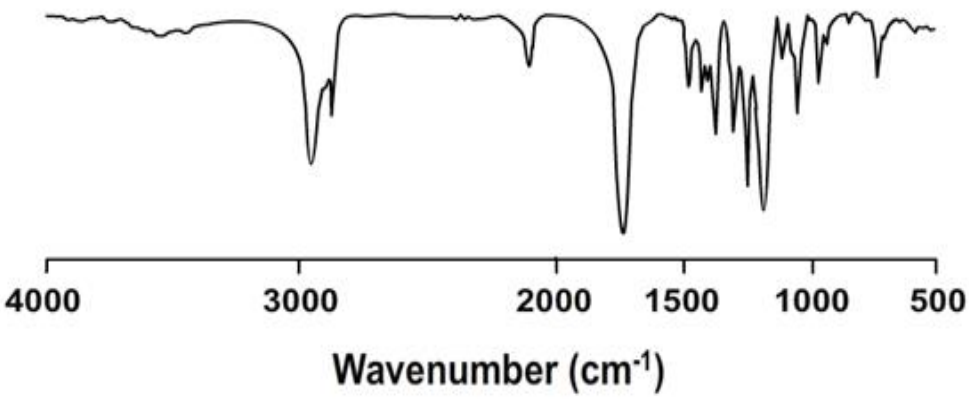

Figure 2.2 IR spectrum of N_3-PCL (KBr).

Figure 2.3 shows ^1H NMR spectrum of N_3-PCL in $CDCl_3$. Small absorptions due to the terminal moieties at α- and ω-ends are clearly observed. The peaks at 3.7 (peak o) and 3.3 (peak a) ppm are due to methylene protons of -C*H*$_2$-OH and –C*H*$_2$-N_3, respectively. These results are a proof of successful introduction of azide group into PCL chains.

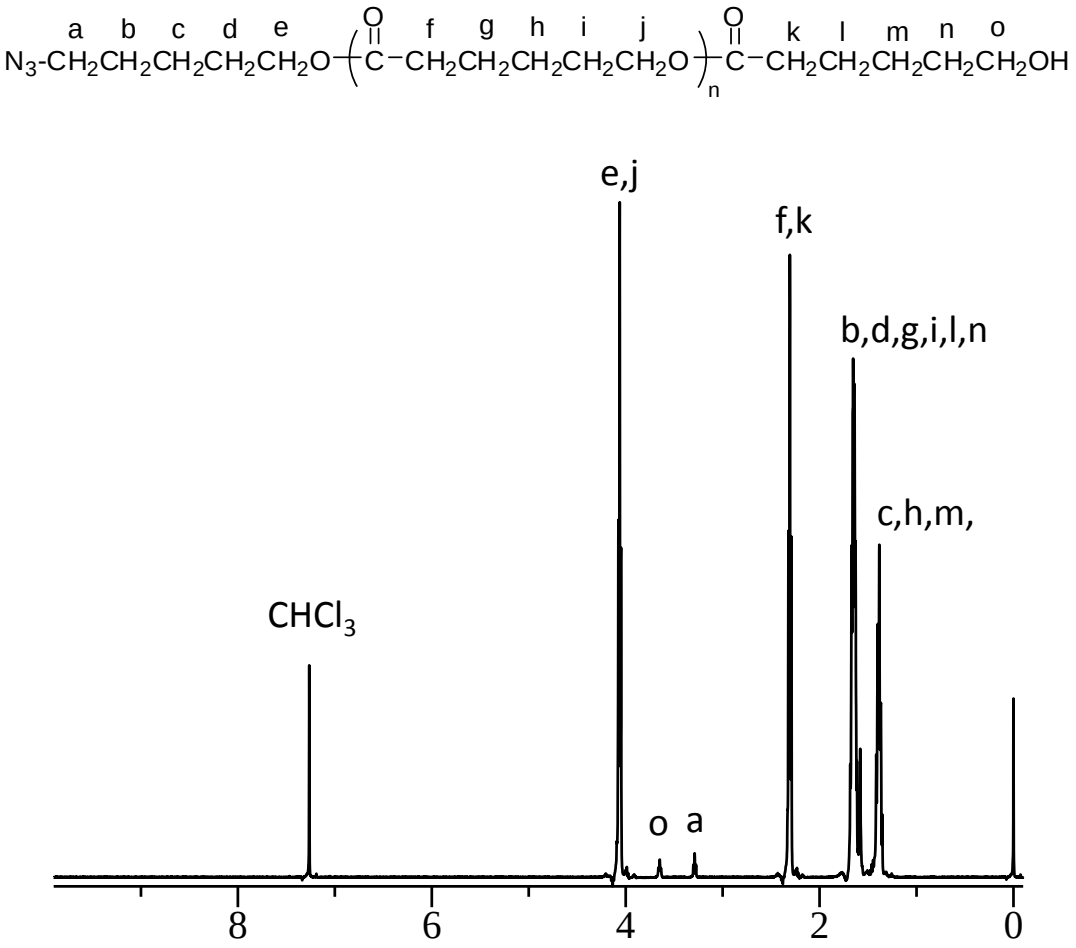

Figure 2.3 ^{1}H NMR spectrum of N_3-PCL.

Exfoliated Graphene Flakes (GFs)

Liquid-phase exfoliation of graphene with the aid of ultrasonication is a convenient method because large-scale production of exfoliated graphene is possible. Khan et al. reported solvent-exfoliated graphene at extremely high concentration in NMP.[26] Shen et al. carried out ultrasonication of pristine graphene in an aqueous PVA solution.[27] PVA macroradicals generated during sonochemical degradation of the PVA solution can be bound to graphene surface to prevent restacking. Preliminary experiment was simultaneous exfoliation and grafting-on reaction. However, the attempt to introduce PCL macromolecules onto GFs by

ultrasonication treatment of GNPs in the presence of N_3-PCL failed. It was found that PCL underwent severe decomposition during ultrasonication process to give complex reaction products. Alternatively, grafting-on reaction was carried out by the reaction of N_3-PCL with the isolated ultrasonication-assisted exfoliated GFs which was prepared according to the method described in Chapter 1.

Functionalization of GFs with Well-Defined N_3-PCL

Grafting of PCL chains onto GFs ([2+1]cycloaddition) was carried out simply by heating the mixture of GFs and N_3-PCL in NMP at 160 ºC under nitrogen atmosphere. The crude product was obtained by precipitation into IPE. To remove unreacted N_3-PCL, the crude product was then precipitated in ether because N_3-PCL is soluble in ether. Purified PCL-*g*-GFs were obtained as the sediment after centrifugation as a dark brown solid. Figure 2.4 shows GPC traces of N_3-PCL and PCL-*g*-GFs. PCL-*g*-GFs showed a unimodal GPC curve that shifted from 3000 to 12000 after grafting reaction. This increase of molecular weight can be explained by the attachment of PCL chains onto GFs. The GPC curve of PCL-*g*-GFs did not contain low molecular weight fraction, indicating that PCL-*g*-GFs were obtained without contamination of unreacted N_3-PCL. The reason for the narrower molecular weight distribution of PCL-*g*-GFs than that of N_3-PCL may be fractionation during repeated precipitation process.

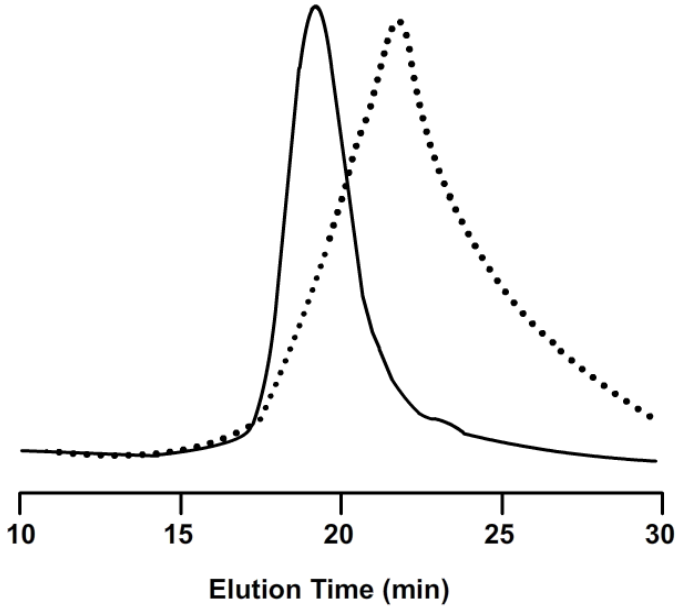

Figure 2.4 GPC traces of N_3-PCL (dotted line) and PCL-*g*-GFs (solid line).

Figure 2.5 shows ^{1}H NMR spectra of N_3-PCL and PCL-*g*-GFs in $CDCl_3$. In addition to absorptions due to PCL main chains, small absorptions due to the terminal moieties at α- and ω-ends are clearly observed. The peaks at 3.7 (peak a) and 3.3 (peak b) ppm are due to methylene protons of -CH_2-OH and –CH_2-N_3, respectively (Figure 2.5a). After reaction with GFs, the peak at 3.3 ppm due to methylene protons next to azido groups disappeared completely. On the other hand, the methylene protons next to terminal hydroxyl group remained (Figure 2.5b). These observations indicated successful introduction of PCL chains onto GFs (Scheme 2.2).

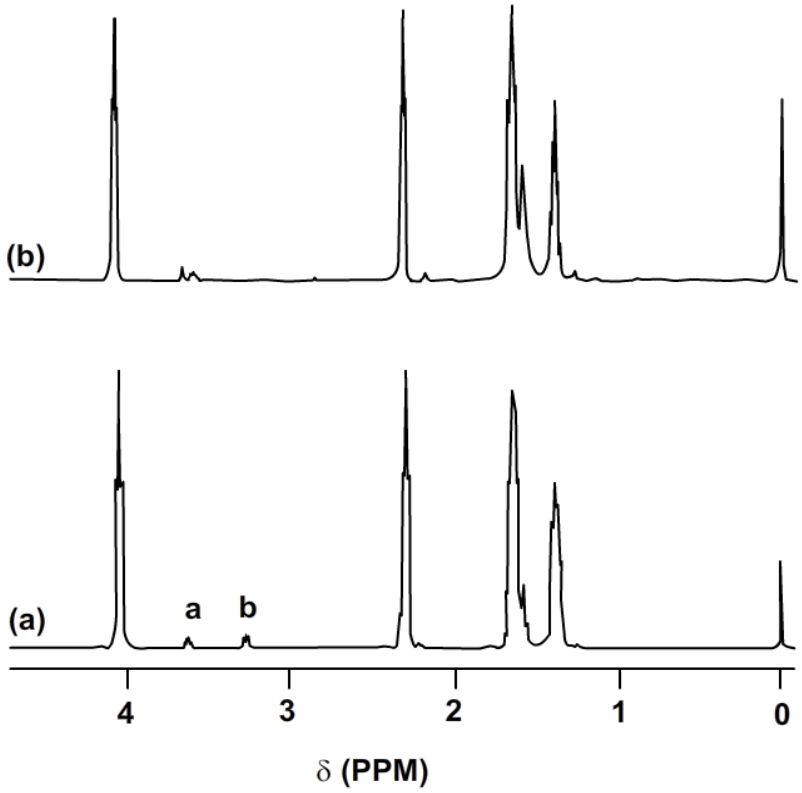

Figure 2.5 ^{1}H NMR spectra of (a) before and (b) after grafting-on reaction.

Figure 2.6 shows IR spectra of PCL-*g*-GFs, N_3-PCL, and GFs. N_3-PCL exhibited a characteristic absorption peak at 2100 cm^{-1} due to the azide groups (Figure 2.6a). GFs do not possess any characteristic fingerprint modes in the absorption spectrum (Figure 2.6b). After reaction with N_3-PCL, characteristic absorption peaks due to PCL moiety were clearly observed at 2946 (ν_{C-H}), 2864 (ν_{C-H}), 1730 ($\nu_{C=O}$), and 1185 cm^{-1} (ν_{C-O}). On the other hand, the absorption at 2100 cm^{-1} due to azido groups disappeared completely, indicating a complete conversion of azido precursor to nitrene (Figure 2.6c).

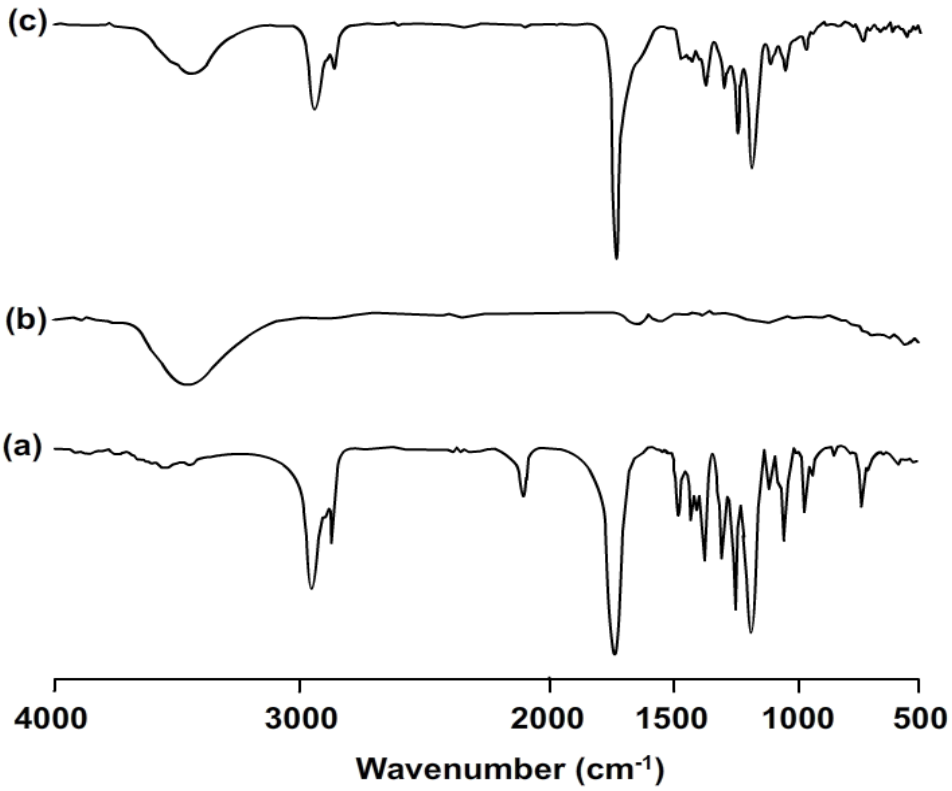

Figure 2.6 IR spectra of (a) N_3-PCL, (b) exfoliated GFs, and (c) PCL-*g*-GFs.

Raman spectroscopic analysis was employed to provide additional structural information on successful grafting of PCL chains onto GFs in the region 1200-2000 cm^{-1} as shown in Figure 2.7. The spectrum of GFs was composed of D (1355 cm^{-1}) and G (1580 cm^{-1}) bands, similar to the Raman spectra of high-quality GFs obtained from liquid phase exfoliation of graphite.[28,29] Apparently, these two peaks were broadened in the spectrum of PCL-*g*-GFs. This peak broadening is probably associated with some structural changes in sp^2 conjugated carbon due to covalent bond formation with PCL macromolecules. It was noted that new peak emerged at 1430 cm^{-1} after functionalization. This peak can be assigned to PCL introduced on GFs because Raman spectrum of PCL is reported to exhibit a strong peak around 1430 cm^{-1}.[30,31]

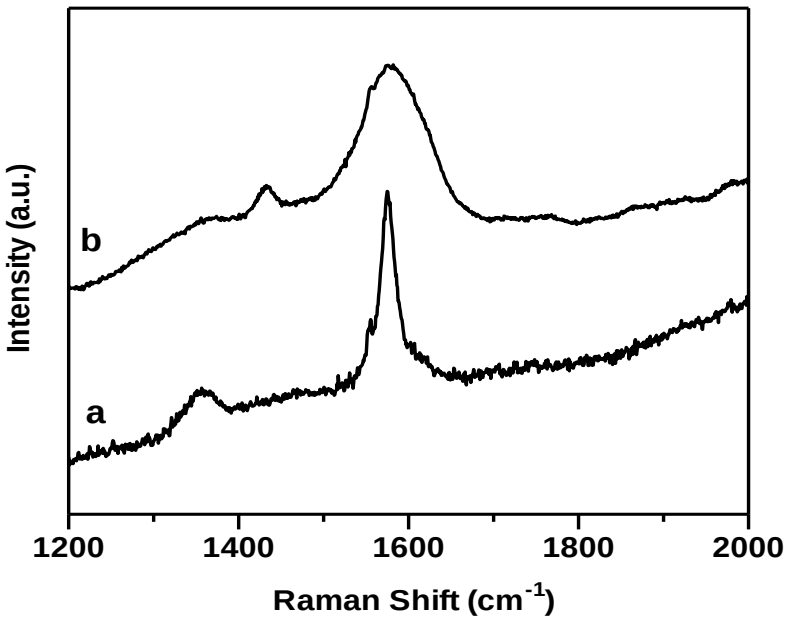

Figure 2.7 Raman spectra of (a) GFs and (b) PCL-*g*-GFs.

In order check the retention of π-conjugated structure of GFs after functionalization, UV-vis analysis was examined. Figure 2.8 shows UV-vis absorption spectra of PCL-*g*-GFs, N_3-PCL, and GFs. N_3-PCL showed strong absorption in the wavelength region shorter than 250 nm, while no evident absorption in the longer wavelength. GFs showed a peak centered at 270 nm with continuously decreasing intensity. It is known that UV-vis spectrum of reduced GO exhibits absorption at 270 nm due to the restoration of electronic conjugation.[32] The absorption of PCL-*g*-GFs still exhibited the characteristic peak at 270 nm. These experimental results indicate that PCL chains were attached on the surface of GFs without disrupting the electronic conjugation structure of GFs.

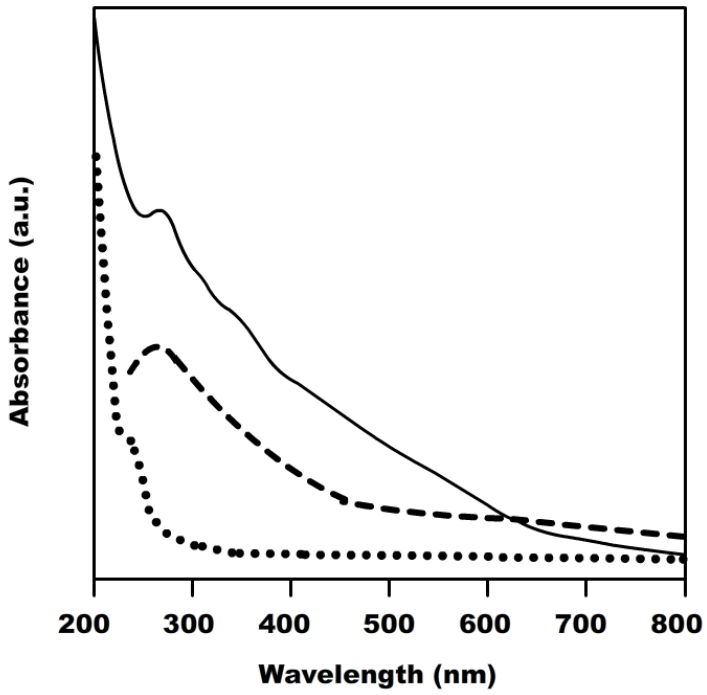

Figure 2.8 UV-vis spectra of N_3-PCL in CH_3CN (dotted line), GFs (dashed line), and thin film of PCL-*g*-GFs (solid line).

The relative amounts of the grafted PCL chains on GFs were determined by TGA analysis. Figure 2.9 shows the TGA thermograms of GFs, N_3-PCL, and PCL-*g*-GFs under nitrogen atmosphere at the heating rate of 10 K/min. The overall weight loss of GFs was about 8% at 1000 °C, showing its good thermal stability (dashed line). In the case of N_3-PCL, significant weight loss started at 270 °C, and finally all PCL burned out at 500 °C (dotted line). Since all of the grafted polymers are assumed to be lost at 500 °C, the weight fraction of the PCL macromolecules in PCL-*g*-GFs was determined to be 75% (solid line).

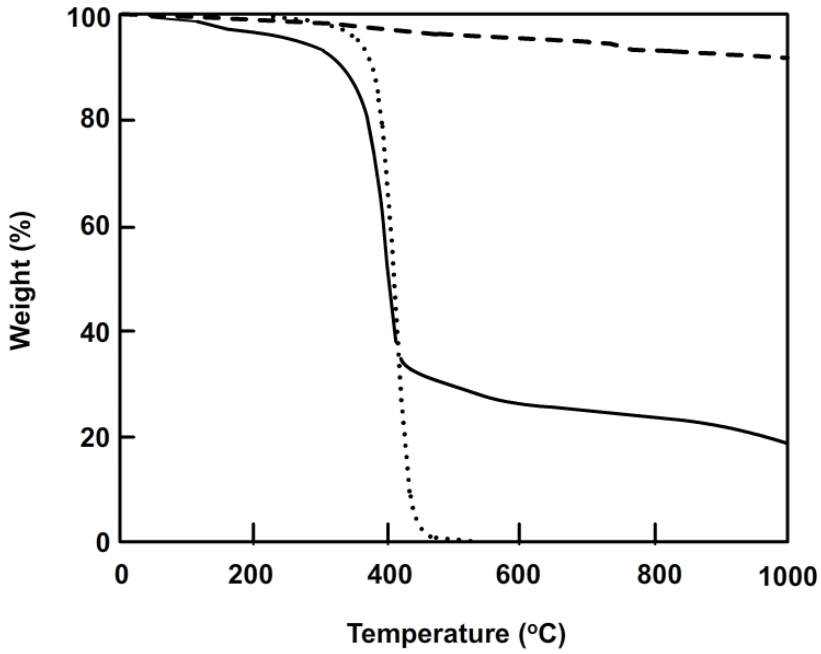

Figure 2.9 TGA curves of GFs (dashed line), N_3-PCL (dotted line), and PCL-*g*-GFs (solid line).

TEM is a powerful tool to visually characterize the morphology of PCL-*g*-GFs. The samples were prepared by placing few drops of diluted dispersion onto carbon grids. Figure 2.10a shows TEM image and SAED pattern of pristine unmodified GFs (inset a). The image of PCL-*g*-GFs exhibited an average lateral size was found to be 1 µm. The SAED exhibited a single set of hexagonal diffraction pattern with sharp and clear diffraction spots, indicating the high crystallinity of the graphene sheets. Figure 2.10b shows representative example of PCL-*g*-GFs. The dark regions are related to the grafted PCL chains onto the surface of GFs. It was worth mentioning that the morphology of GFs did not change significantly after modification with PCL.

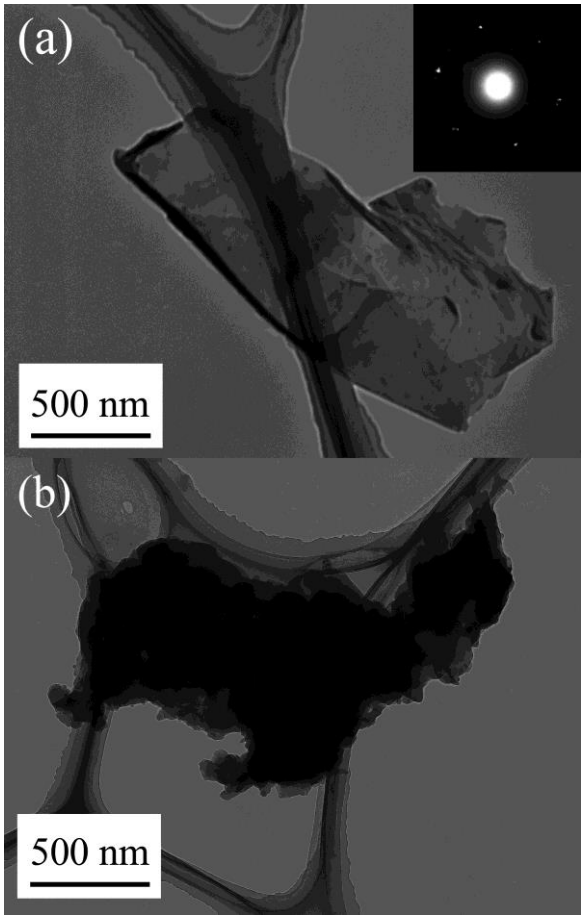

Figure 2.10 TEM images of (a) GFs and (b) representative example of PCL-*g*-GFs.

Table 2.1 summarizes dispersibility of PCL-*g*-GFs in various organic solvents. A small amount (ca. 1 mg) of PCL-*g*-GFs was added to 2 mL of solvents. Excellent dispersion was observed for dichloromethane, THF, benzene, and NMP. On the other hand, sedimentation of black powder at the bottom was observed for methanol and hexane (Figure 2.11). For reference, solubility of N_3-PCL is also summarized in Table 2.1. The dispersibility of PCL-*g*-GFs was reasonably explained by the solubility of the attached PCL. About 75 wt% grafting of PCL chains onto GFs was enough to improve the solubility of GFs.

Table 2.1 Dispersibility of PCL-*g*-GFs and Solubility of N_3-PCL in Various Solvents

solvent	Dispersibility of PCL-*g*-GFs	Solubility of N_3-PCL
hexane	poor	poor
benzene	good	good
CH_2Cl_2	good	good
THF	good	good
NMP	good	good
CH_3OH	poor	poor

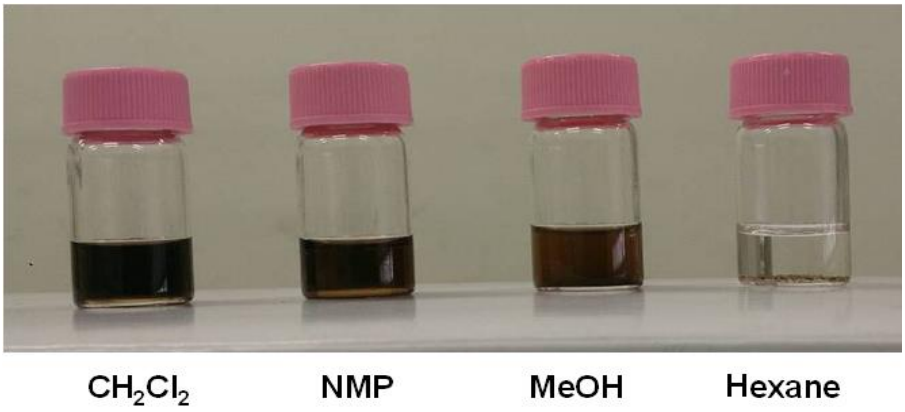

Figure 2.11 Photographs of PCL-*g*-GFs in various solvents

2.5 Conclusion

Functionalization of multi-layered graphene flakes with pre-synthesized well-defined PCL macromolecules was carried out utilizing nitrene chemistry to provide solubility in various organic solvents. GPC, ^{1}H NMR, IR, Raman analysis indicated that PCL chains were successfully introduced onto the surface of GFs through covalent bond formation ([2+1]cycloaddition). TEM and UV-vis measurements revealed the successful grafting-on reaction without disrupting the electronic structure of GFs. Incorporation of 75wt% of PCL macromolecules on GFs was enough to improve the solubility in a wide variety of organic solvents. Soluble GFs composite is expected to find use for solution-based fabrication procedures.

2.6 References

1. K. S. Novoselov, A. K. Geim, S. V. Morozov, D. Jiang, Y. Zhang, S. V. Dubonos, I. V. Grigorieva, A. A. Firsov, *Science* **2004**, *306*, 666–669.

2. A. K. Geim, K. S. Novoselov, *Nat. Mater*. **2007**, *6*, 183–191.

3. C. N. R. Rao, A. K. Sood, K. S. Subrahmanyam, A. Govindaraj, *Angew. Chem., Int. Ed*. **2009**, *48*, 7752–7777.

4. C .N. R. Rao, A. K. Sood, R. Voggu, K. S. Subrahmanyam, *Phys. Chem. Lett*. **2010**, *1*, 572–580.

5. M. J. Allen, V. C. Tung, R. B. Kaner, *Chem. Rev*. **2010**, *110*, 132–145.

6. J. Wu, M. Agrawal, H. A. Becerril, Z. Bao, Z. Liu, Y. Chen, P. Peumans, *ACS Nano* **2010**, *4*, 43–48.

7. X. Wang, L. Zhi, N. Tsao, Ž. Tomović, J. Li, K. Müllen, *Angew. Chem., Int. Ed*. **2008**, *47*, 2990–2992.

8. Z. Chen, M. Zhou, Y. Cao, X. Ai, H. Yang, J. Liu, *Adv. Energy Mater*. **2012**, *2*, 95–102.

9. F. Kokai, R. Sorin, H. Chigusa, K. Hanai, A. Koshio, M. Ishihara, Y. Koga, M. Hasegawa, N. Imanishi, Y. Takeda, *Diamond & Related Mater*. **2012**, *29*, 63–68.

10. D. W. Wang, F. Li, J. Zhao, W. Ren, Z. G. Chen, J. Tan, Z. S. Wu, I. Gentle, G. Q. Lu, H. M. Cheng, *ACS Nano* **2009**, *3*, 1745–1752.

11. R. Kou, Y. Shao, D. Wang, M. H. Engelhard, J. H. Kwak, J. Wang, V. V. Viswanathan, C. Wang, Y. Lin, Y. Wang, *Electrochem. Commun*. **2009**, *11*, 954–957.

12. D. Zhao, G. Sheng, C. Chen, X. Wang, *Appl. Catal*. **2012**, *B 111-112* , 303–308.

13. F. Schedin, A. Geim, S. Morozov, E. Hill, P. Blake, M. Katsnelson, K. Novoselov, *Nat. Mater*. **2007**, *6*, 652–655.

14. T. Kuila, S. Bose, A. K. Mishra, P. Khanra, N. H. Kim, J. H. Lee, *Prog. Mater. Sci*. **2012**, *57*, 1056–1105.

15. K. S. Subrahmanyam, A. Ghosh, A. Gomathi, A. Govindaraj, C. N. R. Rao, *Nanosci. Nanotechnol. Lett*. **2009**, *1*, 28–31.

16. H. J. Salavagione, G. Martinez, G. Ellis, *Macrmol. Rapid Commun*. **2011**, *32*, 1771–1789.

17. R. Wang, X. Wang, S. Chen, G. Jiang, *Designed Monomers Polym*. **2012**, *15*, 303–310.

18. P. X. Thinh, C. Basavajara, J. K. Kim, D. S. Huh, *Polym. Compos*. **2012**, *33*, 2159–2167.

19. L. Hua, W. Kai, Y. Inoue, *J. Appl. Polym. Sci*. **2007**, *106*, 1880–1884.

20. J. Han, C. Gao, *Nano-Micro Lett*. **2010**, *2*, 213–226.

21. H. He, C. Gao, *Chem. Mater*. **2010**, *22*, 5054–5064.

22. L. Zhou, C. Gao, D. Zhu, W. Xu, F. F. Chen, A. Palkar, L. Echegoyen, E. S. W. Kong, *Chem. Eur. J*. **2009**, *15*, 1389–1396.

23. S. Nielsen, C. M. Pedersen, S. G. Hansen, M. D. Petersen, S. Sinning, O. Wiborg, H. H. Jensen, M. Bols, *Bioorg. Med. Chem*. **2009**, *17*, 4900–4909.

24. K. Makiguchi, T. Satoh, T. Kakuchi, *Macromolecules* **2011**, *44*, 1999–2005.

25. Y. Li, J. N. Hoskins, S. G. Screerama, S. M. Grayson, *Macromolecules* **2010**, *43*, 6225–6228.

26. U. Khan, H. Porwal, A. O'Neill, K. Nawaz, P. May, J. N. Coleman, *Langmuir* **2011**, *27*, 9077–9082.

27. B. Shen, W. Zhai, D. Lu, J. Wang, W. Zheng, *RSC Advances* **2012**, *2*, 4713–4719.

28. Y. Hernandez, V. Nicolosi, M. Lotya, F. M. Blighe, Z. Sun, S. De, I. T. McGovern, B. Hollnad, M. Bryne, Y. K. Gun'ko, J. J. Boland, P. Niraj, G. Duesberg, S. Krishnamurthy, R. Goodhue, J. Hutchinson, V. Scardaci, A. C. Ferrari, J. N. Colemen, *Nat. Nanotechnol*. **2008**, 3, 563–568.

29. U. Khan, A. O'Neill, M. Lotya, S. De, J. N. Coleman, *Small* **2010**, *6*, 864–2282.

30. S. J. Bae, M. K. Joo, Y. Jeong, S. W. Kim, W.-K. Lee, Y. S. Sohn, B. Jeong, *Macromolecules* **2006**, *39*, 4873-4879.

31. V. Guarino, F. Cause, P. Taddei, M. D. Foggia, G. Ciapetti, D. Martini, C. Fagnano, N. Baldini, L. Ambrosio, *Biomaterials* **2008**, *29*, 3662-3670.

32. E. Y. Choi, T. H. Han, J. Hong, J. E. Kim, S. H. Lee, H. W. Kim, S. O. Kim, *J. Mater. Chem*. **2010**, *20*, 1907-1912.

Chapter 3

Hybridization of Reduced Graphene Oxide with Silica by Using Poly(2-methyl-2-oxazoline) Modified Reduced Graphene Oxide

3.1 Abstract

Amino-terminated poly(2-methyl-2-oxazoline) (PMeOXz-NH_2) was synthesized using the living cationic ring-opening polymerization of 2-methyl-2-oxazoline (MeOXz). PMeOXz chains were introduced onto graphene oxide (GO) by the condensation reaction between GO and PMeOXz-NH_2 to give PMeOXz-grafted GO (PMeOXz-*g*-GO), which was converted to PMeOXz-grafted reduced graphene oxide (PMeOXz-*g*-rGO) by hydrazine reduction. Acid-catalyzed sol-gel method of tetraethoxysilane (TEOS) was carried out in the presence of PMeOXz-*g*-rGO to give a homogeneous PMeOXz-*g*-rGO/SiO_2 hybrid retaining the optical property of rGO.

3.2 Introduction

Hybrid materials are composites consisting of two constituents at the nanometer or molecular level. Sol-gel method is widely used for obtaining various organic/SiO_2 hybrids which combine the advantages of the organic molecules (flexibility, processability, ductility) and the inorganic materials (rigidity, high thermal stability).[1,2] Kubo et al. reported organic/SiO_2 hybrids using π-conjugated polymers as an organic segment by sol-gel method.[3-5] Hydrolysis-condensations of tetraethoxysilane (TEOS) were carried out in the presence of π-conjugated polymers with functionalities that can interact with silica to obtain homogeneous hybrid retaining the properties of π-conjugated polymer embedded in the silica.

Graphene, 2D single layer of carbon atoms with the hexagonal packed structure,[6] has attracted significant attention by worldwide researchers due to its outstanding properties not seen in any other materials as mentioned in previous chapter. The purpose of this work is to hybridize graphene carrying a large conjugated structure as an organic segment with silica. Hybridization of graphene with silica is expected to further widen the applications of graphene. However, 2D structure and huge specific area of graphene made it easy to aggregate, thus limited its application. [7] It is also not easy to prepare graphene/SiO_2 hybrid due to the lack of interaction between the two components. There is no useful functionality on the graphene surface to overcome the phase separation between graphene and silica. Alternatively, graphene oxide (GO), chemically modified forms of graphene, is an attractive nanomaterial because various oxygen functional groups on the GO surface can offer a route for various graphene-based materials.[8] Recently, Zhang and Choi carried out sol-gel reaction of TEOS in the presence of GO to obtain GO/SiO_2 hybrid utilizing strong interaction between silica and functional groups on the GO surface.[9] However, the oxidization process disrupts the sp^2 hybrid carbon network, meaning the loss of the properties of graphene with large π-conjugated structure. Once GO is incorporated into silica, it is difficult to restore graphene from GO because silica hybrid is insoluble and non-swelling.

In this chapter a novel strategy for PMeOXz-*g*-rGO/SiO_2 hybrid will be proposed. The synthetic pathway for PMeOXz-*g*-rGO/SiO_2 hybrid is shown in Scheme 3.1. The idea is covalent modification of rGO with poly(2-methyl-2-oxazoline) (PMeOXz). Since polar polymer such as PMeOXz is known to form a homogeneous hybrid with silica through hydrogen bonding interaction,[10] the introduced PMeOXz chains on the rGO surface can be a useful compatibilizer between rGO and silica. The grafting-on reaction of PMeOXz onto GO to obtain PMeOXz-grafted GO (PMeOXz-*g*-GO), chemical reduction of PMeOX-*g*-GO to PMeOX-*g*-rGO to restore conjugated structure, and the sol-gel method of TEOS in the

presence of PMeOXz-grafted rGO (PMeOXz-*g*-rGO) to obtain PMeOXz-*g*-rGO/SiO_2 hybrid will be described.

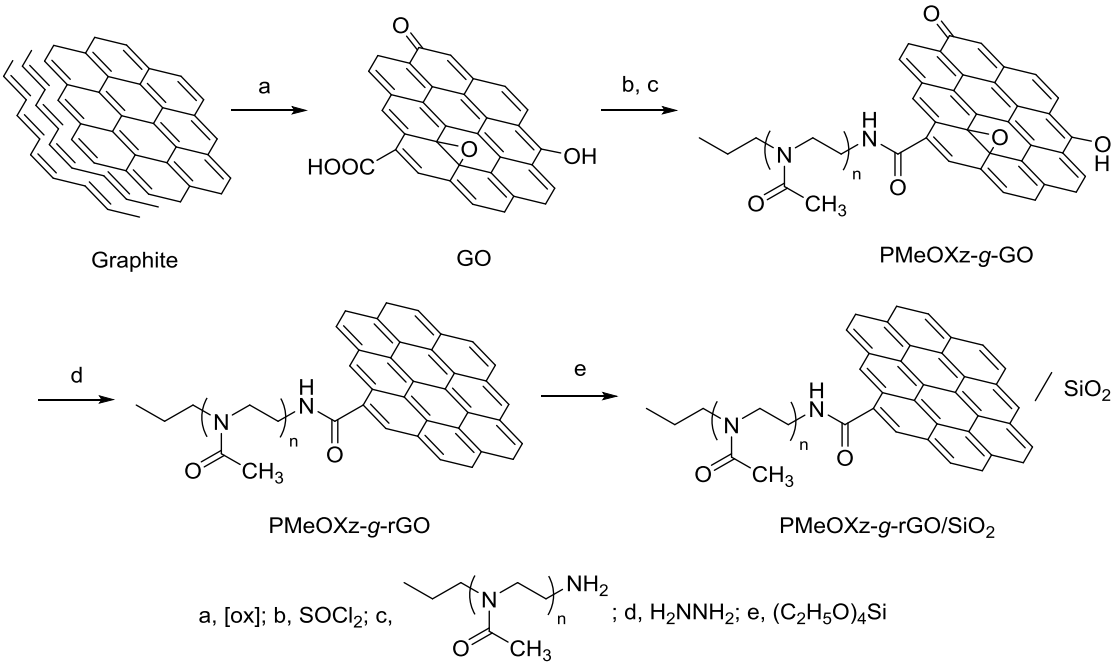

Scheme 3.1 Synthetic route for PMeOXz-*g*-rGO/SiO_2 hybrid.

3.3 Experimental

Materials

Natural graphite (Z-25) was purchased from Ito Graphite Industries. MeOXz and TEOS were purchased from Tokyo Chemical Industry and purified by distillation. All other reagents were purchased from commercial sources and purified by usual methods.

Measurements

^{1}H NMR was recorded at room temperature on a JEOL α-500 nuclear magnetic resonance at 500 MHz. Samples were dissolved in D_2O and sodium 3-(trimethylsilyl)propane-1-sulfonate (DSS) was added as the internal standard. Infrared (IR) and UV-vis spectra were recorded on

a JASCO FT/IR-4100 and Shimadzu UV-2550, respectively. The morphology of the sample was observed using a HITACHI H-7000 transmission electron microscope (TEM) operated at 100 kV. Scanning electron microscope (SEM) was observed using a HITACHI S4800.

Synthesis of graphene oxide (GO)

GO was prepared by oxidation of graphite followed by the exfoliation of the graphite oxide using repetitive simple freeze-thaw cycles according to the reported procedure.[11] Typically, 0.30 g of $NaNO_3$ and 0.60 g of natural graphite were placed in a 100 mL Erlenmeyer flask with a Teflon-coated stir bar with a length of 30 mm. To this mixture was added 13.8 mL of H_2SO_4, and the mixture was cooled to 0 ºC using an ice-water bath. To the slurry was slowly added 1.8 g of $KMnO_4$ to keep the temperature of the mixture below 20 ºC. After the addition of $KMnO_4$, the temperature of the mixture was increased to 35 ºC and held for 30 min while the mixture was vigorously stirred. Deionized water (28 mL) was added dropwise to this mixture, and the temperature of the mixture was increased to 98 ºC and held for 30 min. The mixture was cooled using an ice-water bath for 10 min. Then, 0.60 mL of 30% H_2O_2 and 84 mL of deionized water were added to the mixture. After cooling at room temperature, the mixture was centrifuged at 3000 rpm for 5 min, and the supernatant solution was discarded. The remaining solid was washed with approximately 170 mL of deionized water a total of five times. The solid was collected by centrifugation and dried in vacuum to obtain graphite oxide. Then, the ground graphite oxide (10 mg) and deionized water (5 mL) were placed in a polypropyrene tube (12 mm in diameter and 140 mm in length) and soaked in a liquid nitrogen bath. After the mixture was completely frozen, the tube was soaked in a thermostated bath at 60 ºC for 10−20 min to thaw the solid. Then, the mixture was centrifuged at 3000 rpm for 5 min, and an aliquot of the supernatant solution was withdrawn for UV−vis characterization. This freeze−thaw cycle was repeated six times.

Synthesis of amino-terminated poly(2-methyl-2-oxazoline) (PMeOXz-NH_2)

To the solution of MeOXz (2.0 g, 24 mmol) in 10 mL of acetonitrile was added 1-iodopropane (70 μL, 0.72 mmol) and the mixture was stirred under reflux for 24 h. After cooling to 0 ºC, ammonia gas was bubbled for 30 min and the mixture was stirred at room temperature for 24 h. The polymer was purified by precipitation in ether to give 2.1 g (quant) of PMeOXz-NH_2 as white solid.

Synthesis of PMeOXz-g-GO

The mixture of GO (20 mg), $SOCl_2$ (20 mL), and *N*,*N*-dimethylformamide (DMF) (0.5 mL) was refluxed under nitrogen for 24 h to convert -COOH to -COCl. Excess $SOCl_2$ and the solvent were removed under vacuum. To the residue were added DMF (10 mL), triethylamine (0.5 mL), and PMeOXz-NH_2 (40 mg) and the mixture was stirred at 80 ºC for 72 h. The reaction mixture was filtered with TEFLON filter (0.45μ m) to remove unreacted GO and poured into ether to precipitate 70 mg of PMeOXz-*g*-GO as a brownish hygroscopic powder.

Synthesis of PMeOXz-g-rGO

The mixture of PMeOXz-*g*-GO (70 mg), water (10 mL), and hydrazine hydrate (10 μL) was heated at 95 ºC for 18 h. Freeze-drying of the reaction mixture gave 38 mg of PMeOXz-*g*-rGO as a brownish hygroscopic powder.

Synthesis of unmodified rGO

Unmodified rGO without PMeOXz chains was prepared for control experiment. A mixture of GO (20 mg), water (6 mL), and hydrazine hydrate (10 μL) was heated at 95 ºC for 18 h. After reaction, water (50 mL) was added to the reaction mixture, and the mixture was

centrifuged for 10 min at 2500 rpm. The sediment was dried in vacuo to give 13 mg of unmodified rGO as a black powder.

Sol-gel method

Given amounts of TEOS, PMeOXz-*g*-rGO or rGO, methanol, and 0.1M hydrochloric acid were mixed with stirring in a vial. The reaction mixture was stirred for 30 min at room temperature, spin-coated on a glass plate, and allowed to stand at room temperature.

3.4 Results and Discussion

Synthesis of GO

GO is typically synthesized by oxidizing graphite by using either Hummers' method or Brodie's method,[12,13] followed by subsequent exfoliation of the resultant graphite oxide. The most common technique for exfoliation of graphite oxide is sonication. However, as in the case of exfoliation of other types of layered materials, sonication treatment sometimes reduces the size of the resulting GO sheets. In this work we exfoliated graphite oxide by the freeze-thaw process without sonication reported by Ogino et al.[11] Because the simple method can achieve a high GO yield (~80% after six cycles of the freeze−thaw process) and virtually retains the original nanosheet size. Figure 3.1 shows the UV-vis spectra of exfoliated GO. GO possess two characteristic absorption bands at 230 nm and 300 nm, corresponding to π-π* transitions of aromatic C=C bonds and n→ π* of C=O bonds as peak and shoulder, respectively.[14] These bands increased as the freeze-thaw cycle was repeated which indicates an increased concentration of dispersed GO.

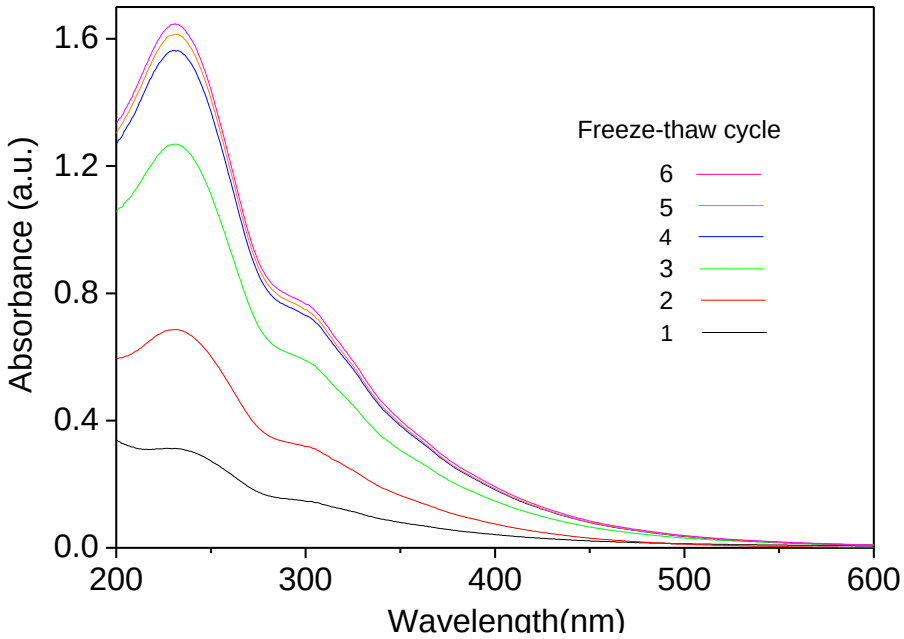

Figure 3.1 UV-Vis spectra of exfoliated GO.

The morphology of the formed GO was investigated by TEM observation. Figure 3.2 shows a TEM image and selected area electron diffraction (SAED) pattern of GO used in this study. The sheet is so thin that electron beam can be passed through the sample. The SAED patterns exhibited several sets of hexagonal diffraction patterns, indicating a multi-layered structure.

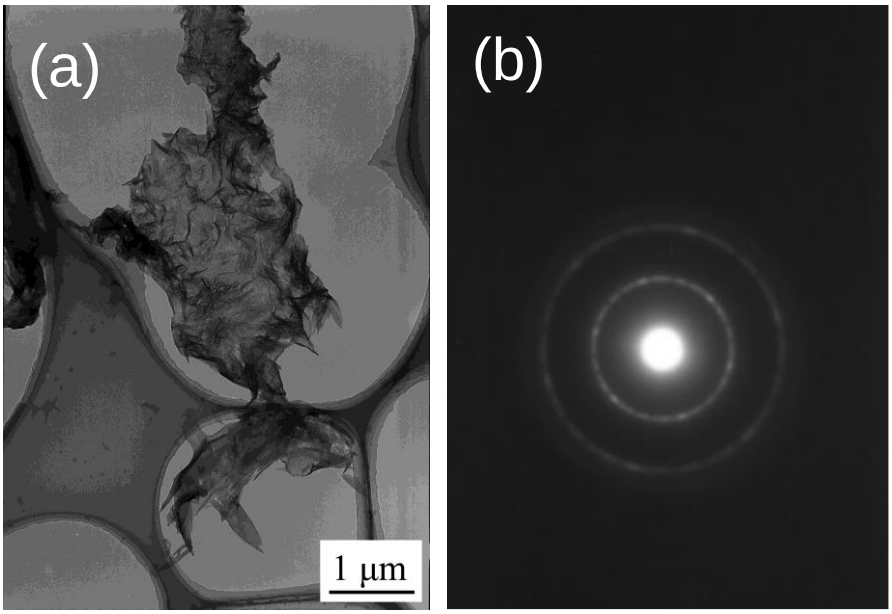

Figure 3.2 TEM image (a) and selected area electron diffraction (SAED) pattern (b) of GO.

Synthesis of PMeOXz-NH_2

We are interested in PMeOXz as a polymer segment to be attached onto rGO because PMeOXz is known to be miscible with silica by sol-gel method due to the existence of hydrogen bonding between them.[10] Amino-terminated PMeOXz was prepared by the living cationic ring-opening polymerization of MeOXz according to the reported procedures[15,16] (Scheme 3.2). The degree of polymerization was designed to be around 30. These relatively short polymer chains should be sufficient to control the solubility of the attached rGO. Moreover, the low molecular weight simplifies the characterizations such as IR and NMR. Fig. 3.3 shows ^{1}H NMR spectrum of PMeOXz-NH_2 in D_2O. The number-average degree of polymerization (n) was determined by the ratio of the peak area of CH_3 protons of repeating unit (a) to that of terminal CH_3 protons (d). The obtained value (32) was in good agreement with the calculated value (33) from the molar feed ratio of MeOXz monomer to iodopropane.

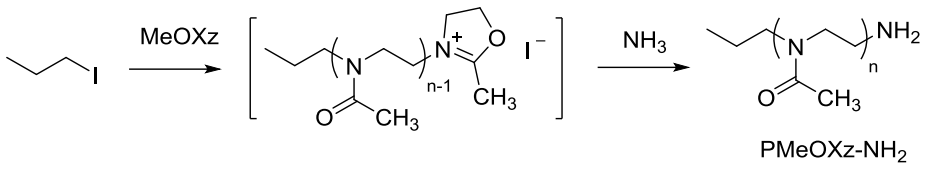

Scheme 3.2 Synthesis of amino-terminated poly(2-methyl-2-oxazoline) (PMeOXz-NH_2).

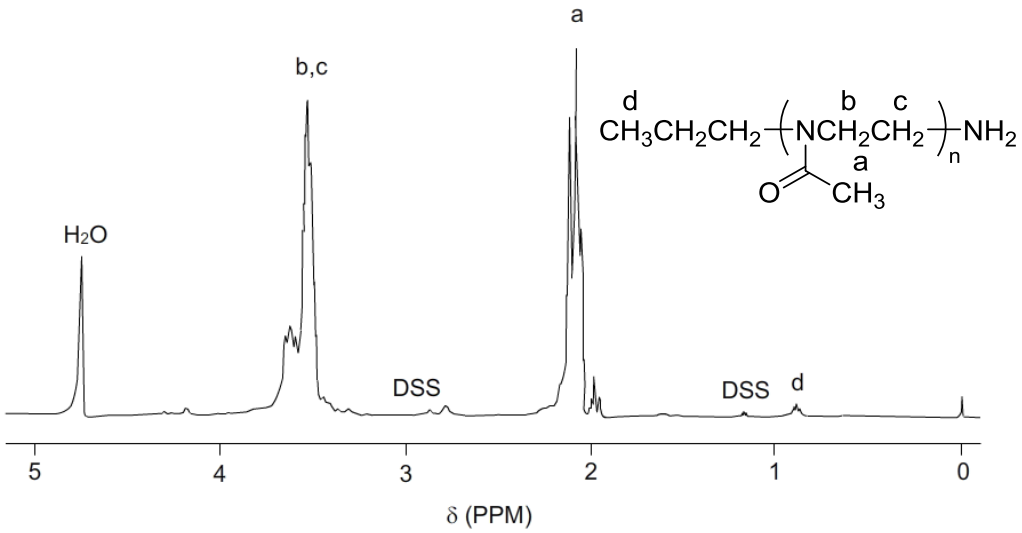

Figure 3.3 ^{1}H NMR of PMeOXz-NH_2 in D_2O.

Grafting of PMeOXz-NH_2 onto GO

Grafting of PMeOXz-NH_2 onto GO was carried out using a standard chemistry. The carboxyl functionalities on the GO surface were converted to acid chloride,[17] and then reacted with PMeOXz-NH_2 to covalently immobilize PMeOXz chains onto GO through amide linkage. Figure 3.4 shows IR spectra of GO, PMeOXz-NH_2, and PMeOXz-*g*-GO. GO exhibited characteristic absorptions at 1725 and 1080 cm^{-1} due to stretching vibrations from C=O and C-O stretching vibrations, respectively (Figure 3.4a). The absorption spectrum of PMeOXz-*g*-GO contained the characteristic peaks of both GO and PMeOXz-NH_2 (Figure

3.4c). Figure 3.5 shows UV-vis spectra of GO, PMeOXz-NH_2, and PMeOXz-*g*-GO in solution state. The absorption at 230 nm observed for GO is known to be characteristic for exfoliated GO (Figure 3.5a). PMeOXz-*g*-GO exhibited both characteristic absorptions of GO and PMeOXz-NH_2 (Figure 3.5c). These results suggest a successful grafting of PMeOXz chains onto GO surface. To check the physical absorption of unreacted free PMeOXz-NH_2 chains on the GO surface, we examined ninhydrin test. Ninhydrin (2,2-dihydroxyindane-1,3-dione) is a useful chemical to detect primary amines. When reacting with free amines, a deep blue or purple color known as Ruhemann's purple is produced. Actually, a deep purple coloring was observed for PMeOXz-NH_2. On the other hand, coloring did not take place for PMeOXz-*g*-GO, indicating that the resulting PMeOXz-*g*-GO was not contaminated with unreacted free PMeOXz chains. The morphology of the resulting PMeOXz-*g*-GO was investigated by TEM observation. Figure 3.6a shows a representative example of PMeOXz-*g*-GO. The dark regions are related to the grafted PMeOXz chains onto the surface of GO.

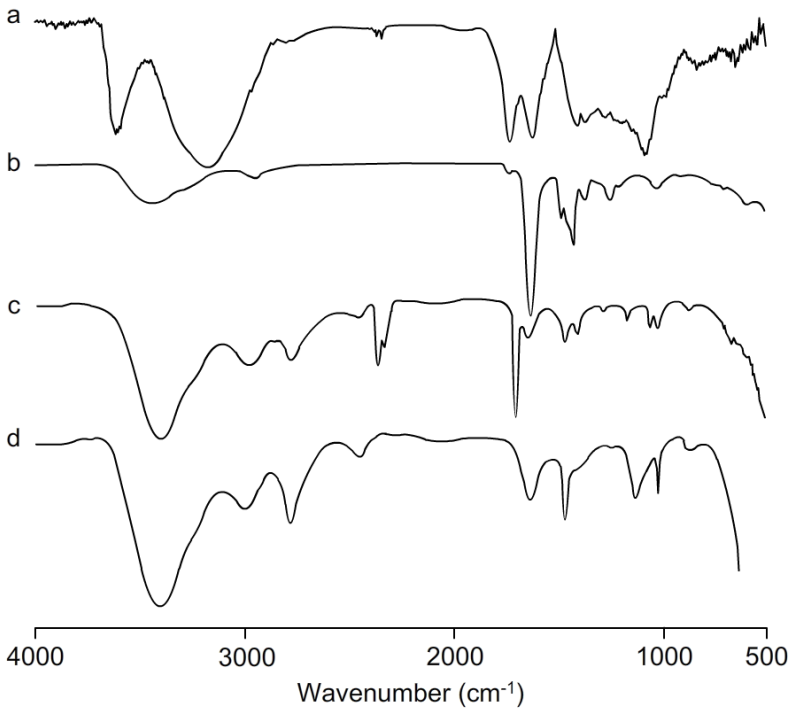

Figure 3.4 IR spectra of (a) GO, (b) PMeOXz-NH_2, (c) PMeOXz-*g*-GO, and (d) PMeOXz-*g*-rGO.

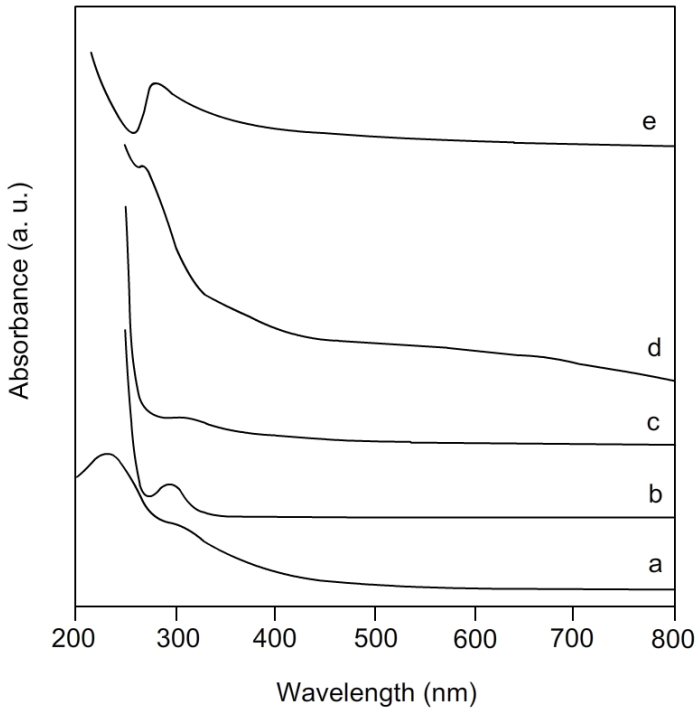

Figure 3.5 UV-vis spectra of (a) GO, (b) PMeOXz-NH_2, (c) PMeOXz-*g*-GO, (d) PMeOXz-*g*-rGO, and (e) PMeOXz-*g*-rGO/SiO_2 hybrid obtained from run 3 (Table 3.1)

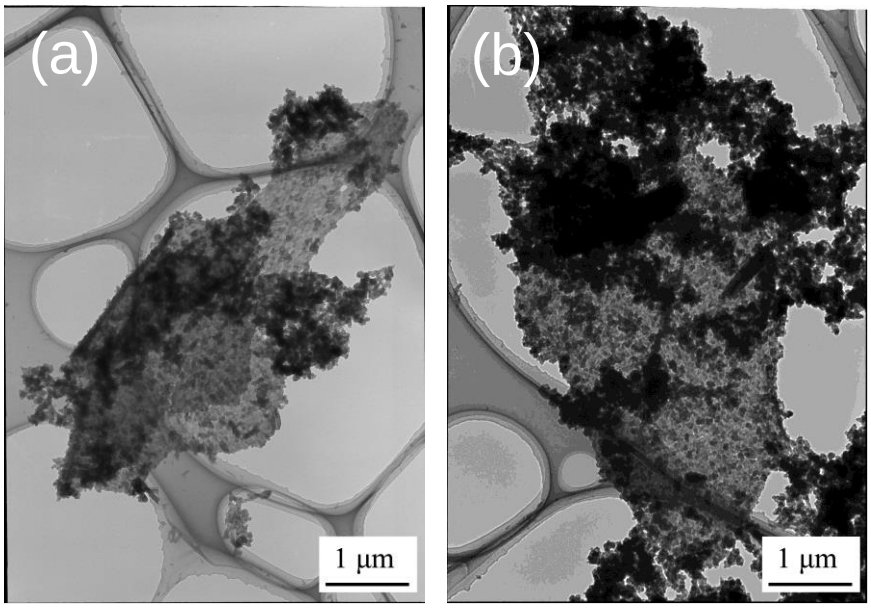

Figure 3.6 TEM images of (a) PMeOXz-*g*-GO and (b) PMeOXz-*g*-rGO

Reduction of PMeOXz-g-GO

Restoration of graphene with π–conjugated structure can be achieved by the reduction of GO. There are a number of routes for reduction of GO.[18,19] The choice of the reduction method in this study was chemical reduction using hydrazine because amide linkage is inert during hydrazine reduction. After treatment with hydrazine the peak at 1725 cm^{-1} due to C=O (ketone) groups of GO disappeared. While, the peak at 1630 cm^{-1} due to C=O (amide) groups of PMeOXz segment was still observed (Figure 3.4d). Restoration of π–conjugated structure was also confirmed by UV-vis absorption spectrum as shown in Figure 3.5d. The observed red shift of π-π* transition from 230 nm to 280 nm is attributable to the electronic conjugation within the rGO sheets. TEM observation showed that PMeOXz chains still remained unchanged on the surface of rGO (Figure 3.6b), indicating that cleavage of PMeOXz chains from rGO surface did not take place during hydrazine treatment. Further, it is worth mentioning that the morphology of GO did not change significantly after reduction.

Synthesis of PMeOXz-g-rGO/SiO_2

The well-known sol-gel method was employed to fabricate PMeOXz-*g*-rGO/SiO_2 hybrid. The acid-catalyzed hydrolysis and polycondensation of TEOS were carried out in the presence of PMeOXz-*g*-rGO. For controlled experiment, similar sol-gel reaction was carried out using unmodified rGO instead of PMeOXz-*g*-rGO. The results are summarized in Table 3.1. The sample using rGO without PMeOXz chains showed phase separation resulting from the aggregation of rGO in the silica matrix, because there is no interaction between rGO and silica (run 1). On the other hand, introduction of PMeOXz chains onto rGO was effective for homogeneous hybrid formation (runs 2 and 3). This indicates that hydrogen bonding between silanol groups and PMeOXz played an important role in increasing the compatibility between rGO and silica. Photographs of the reaction products are shown in Figure 3.7.

Figure 3.8 shows SEM image of the transparent hybrid obtained from run 3, indicating homogeneous dispersion of PMeOXz-*g*-rGO in the silica matrix.

Table 3.1 Results of sol-gel method[a]

run	organic segment (mg)	TEOS, g	CH_3OH, mL	appearance
1	rGO (1)	0.25	2.7	phase separation
2	PMeOXz-*g*-rGO (1)	0.25	2.7	homogeneous
3	PMeOXz-*g* rGO (10)	0.25	2.7	homogeneous

[a] 0.1M Hydrochloric acid, 100 μL.

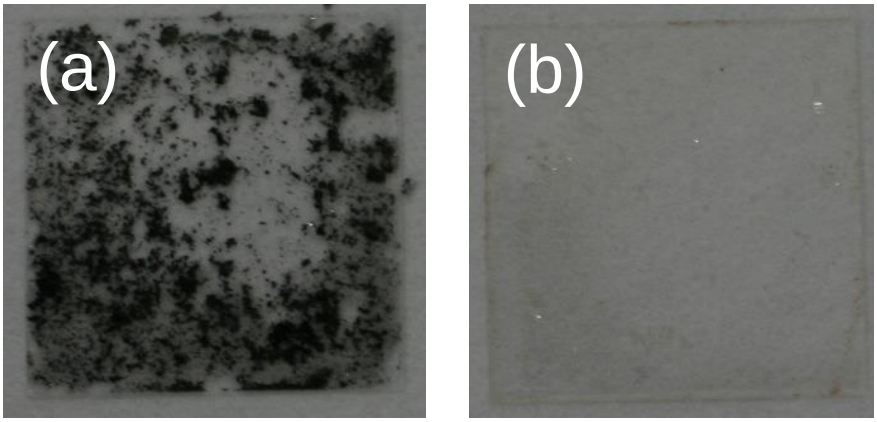

Figure 3.7 Photographs of reaction products obtained from run 1 (a) and run 3 (b).

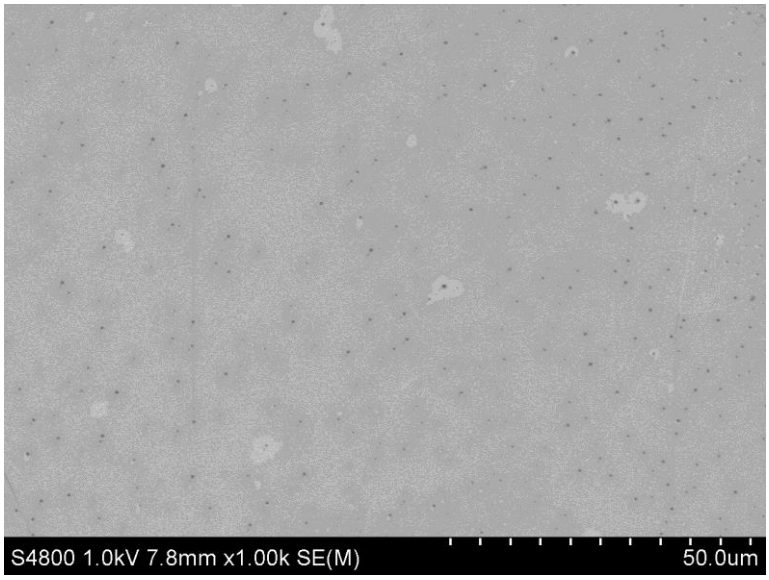

Figure 3.8 SEM image of reaction product obtained from run 3.

Finally, retention of π-conjugated structure of rGO after hybrid formation with silica was examined by UV-vis measurement. The UV-vis spectrum of PMeOXz-*g*-rGO/SiO_2 hybrid (obtained from run 3) exhibited a peak at 280 nm which is characteristic for rGO (Figure 3.4e). It is safe to conclude that rGO was successfully incorporated into silica retaining its optical property.

3.5 Conclusions

A novel strategy for the preparation of homogeneous silica hybrid with rGO was demonstrated. Firstly, PMeOXz macromolecules with terminal amine functionality were covalently attached by grafting-on method onto GO surface through amide linkage to obtain PMeOXz-*g*-GO. Secondly, PMeOXz-*g*-GO was converted to PMeOXz-*g*-rGO by chemical reduction of PMeOXz-*g*-GO using hydrazine treatment. Lastly, conventional sol-gel reaction of TEOS was carried out in the presence of PMeOXz-*g*-rGO to obtain a homogeneous

PMeOXz-*g*-rGO/SiO_2 hybrid. The resulting hybrid exhibited optical property of rGO, indicating retention of conjugated structure of rGO. Homogeneous hybridization of PMeOXz-*g*-rGO with silica is expected to offer strong and tough materials for various applications.

3.6 References

1. B. M. Novak, *Adv. Mater*. **1993**, *5*, 422-433.
2. J. Wen, G. L. Wilkes, *Chem. Mater.* **1996**, *8*, 1667-1681.
3. M. Kubo, C. Takimoto, Y. Minami, T. Uno, T. Itoh, M. Shoyama, *Macromolecules* **2005**, *38*, 7314-7320.
4. Y. Sugiura, M. Shoyama, K. Inoue, T. Uno, T. Itoh, M. Kubo, *Polym. Bull*. **2006**, *57*, 865-871.
5. A. Miyao, Y. Mori, T. Uno, T. Itoh, T. Yamasaki, A. Koshio, M. Kubo, *J. Polym. Sci: Part A: Polym. Chem*. **2010**, *48*, 5322-5328.
6. J. Hass , W. A. de Heer , E. H. Conrad , *J. Phys.: Condens. Matter.* **2008** , *20* , 323202-3232208 .
7. L. Y. Hao, H. J. Song, L. C. Zhang, X. Y. Wan, Y. R. Tang, Y. Lv, *J. Colloid Interface Sci.* **2012**, *369*, 381-387
8. J. Shen, Y. Hu, M. Shi, X. Lu, C. Qin, C. Li, M. Ye, *Chem. Mater*. **2009**, *21*, 3514-3520.
9. W. L. Zhang, H. J. Choi, *Langmuir* **2012**, *28*, 7055-7062.
10. T. Ogoshi, Y. Chujo Y, *Polymer* **2006**, *47*, 4036-4041.

11. I. Ogino, Y. Yokoyama, S. Iwamura, S. R. Mukai, *Chem. Mater*. **2014**, *26*, 3334-3339.

12. B. C. Brodie, *Phi. Trans. R. Soc. Lond*. **1859**, *149*, 249-259.

13. W. S. Hummers, R. E. Offeman, *J. Am. Chem. Soc*. **1958**, *80*, 1339.

14. J. I. Paredes, S. Villar-Rodil, A. Martínez-Alonso, J. M. D. Tascón, *Langmuir* **2008**, *24* , 10560−10564.

15. S. Kobayashi, E. Masuda, S. I. Shoda, Y. Shimano, *Macromolecules* **1989**, *22*, 2878-2884.

16. G. Volet, T. X. Lav, J. Babinot, C. Amiel, *Macromol. Chem. Phy*. **2011**, *212*, 118-124.

17. Y. Xu, Z. Liu, X. Zhang, Y. Wang, J. Tian, Y. Huang, Y. Ma, X. Zhang, Y. Chen, *Adv. Mater*. **2009**, *21*, 1275-1279.

18. S. Park, R. S. Ruoff. *Nat. Nanotechnol*. **2009**, *4*, 217-224.

19. K. P. Loh, Q. Bao, P. K. Ang, J. Yang J, *J. Mater. Chem*. **2010**, *20*, 2277-2289.

ACKNOWLEDGEMENTS

I would like to give my deepest appreciation to my supervisor Professor Fumio Kokai who gave me the opportunity to conduct my doctoral studies at Mie University. Special thanks go to Professor Masataka Kubo for his guidance throughout the research work with useful and constructive suggestions and also with my daily life in Japan. Not to mention, Dr. Akira Koshio for helping me out with laboratory works.

My gratitude goes to my lab partner Kazuki Hirata for making this research possible, Daiki Ando and Kazuya Hatano for helping me out with preparation of N_3-PCL and TEM measurement. In addition, Rika Sorin and Katano Takafumi for lend me a hand on preparing graphene flakes.

My appreciation goes to Professor Takahito Itoh, Dr. Takahiro Uno, Masashi Tamura and students of Laser Photochemistry Laboratory and Polymer Synthetic Chemistry Laboratory, for being helpful and also making the working place fun and enjoyable to work at.

My very special appreciation goes to family especially to my parents, Mr. and Mrs. Abdullah, my beloved aunty and parents-in-law for their hearty encouragement.

To my one and only husband, Aminul Hakim, his continued understanding and support throughout the PhD's journey. You are always around at times I thought that it is impossible to continue, you helped me to keep things in perspective even though we are thousands of miles away

Last but not least, my gratitude goes to my sponsor, TATI University College.